Cytokinin inhibits fungal development and virulence by targeting the cytoskeleton and cellular trafficking

Rupali Gupta[1], Gautam Anand[1], Lorena Pizarro[1,2], Dana Laor[3], Neta Kovetz[1], Noa Sela[1], Tal Yehuda[3], Ehud Gazit[3] and Maya Bar[1].

[1]*Department of Plant Pathology and Weed Research, ARO, Volcani Center, Rishon LeZion 7505101, Israel.*

[2]*Institute of Agri-food, Animal and Environmental Sciences, Universidad de O'Higgins, Chile.*

[3]*The Shmunis School of Biomedicine and Cancer Research, Tel Aviv University, Tel Aviv 6997801, Israel.*

Corresponding author: Maya Bar

mayabar@volcani.agri.gov.il

ORCID: 0000-0002-7823-9121

Keywords: cytokinin, cell cycle, cytoskeleton, endocytosis, *Botrytis cinerea*, *Saccharomyces cerevisiae*

Abstract

Cytokinin (CK) is an important plant developmental regulator, having activities in many aspects of plant life and its response to the environment. CKs are involved in diverse processes in the plant, including stem-cell maintenance, vascular differentiation, growth and branching of roots and shoots, leaf senescence, nutrient balance and stress tolerance. In some cases, phytopathogens secrete CKs. It has been suggested that to achieve pathogenesis in the host, CK-secreting biotrophs manipulate CK signaling to regulate the host cell cycle and nutrient allocation. CK is known to induce host plant resistance to several classes of phytopathogens from a handful of works, with induced host immunity *via* salicylic acid signaling suggested to be the prevalent mechanism for this host resistance.

Here, we show that CK directly inhibits the growth, development, and virulence of fungal phytopathogens. Focusing on *Botrytis cinerea (Bc)*, we demonstrate that various aspects of fungal development can be reversibly inhibited by CK. We also found that CK affects both budding and fission yeast in a similar manner. Investigating the mechanism by which CK influences fungal development, we conducted RNA-NGS on mock and CK treated *B. cinerea* samples, finding that CK inhibits the cell cycle, cytoskeleton, and endocytosis. Cell biology experiments demonstrated that CK affects cytoskeleton structure and cellular trafficking in *Bc*, lowering endocytic rates and endomembrane compartment sizes, likely leading to reduced growth rates and arrested developmental programs. Mutant analyses in yeast confirmed that the endocytic pathway is altered by CK .

Our work uncovers a remarkably conserved role for a plant growth hormone in fungal biology, suggesting that pathogen-host interactions resulted in fascinating molecular adaptations on fundamental processes in eukaryotic biology.

Importance

Cytokinins (CKs), important plant growth/ developmental hormones, have previously been associated with host disease resistance. Here, we demonstrate that CK directly inhibits the growth, development, and virulence of *B. cinerea* (*Bc*) and many additional phytopathogenic fungi. Molecular and cellular analyses revealed that CK is not toxic to *Bc*, but rather, *Bc* likely recognizes CK and responds to it, resulting in cell cycle and individual cell growth retardation, via downregulation of cytoskeletal components and endocytic trafficking. Mutant analyses in yeast confirmed that the endocytic pathway is a CK target. Our work demonstrates a conserved role for CK in yeast and fungal biology, suggesting that suggesting that pathogen-host interactions may cause molecular adaptations on fundamental processes in eukaryotic biology.

1   **Introduction**

2   Cytokinins (CKs) are a class of extensively studied plant hormones, well known for their

3   involvement in various aspects of plant life (Mok & Mok, 2001; Sakakibara, 2006; Werner &

4   Schmülling, 2009; Keshishian & Rashotte, 2015). Some findings have suggested a role for CKs

5   in fungal pathogenesis (Walters & McRoberts, 2006; Babosha, 2009; Sharma *et al.*, 2010; Choi

6   *et al.*, 2011). In some cases, plant pathogens can secrete CKs, or induce CK production in the

7   host plant, possibly in order to achieve pathogenesis in the host (Jameson, 2000). Conidia,

8   mycelia of some fungi, and germinating uredospores of *Puccinia graminis* and *P. recondite* have

9   been shown to accumulate CK, manipulating CK signaling to regulate host plant cell cycle

10   (Greene, 1980; Nieto & Frankenberger, 1991).

11   CK has also been shown to promote resistance to plant pathogens that do not secrete CK. High

12   levels of CKs were found to increase the plants' resistance to bacterial and fungal pathogens

13   (Swartzberg *et al.*, 2008; Choi *et al.*, 2010; Grosskinsky *et al.*, 2011; Ballaré, 2011; Gupta *et al.*,

14   2020a,b). Different mechanisms have been suggested for this enhanced resistance. In

15   Arabidopsis, it was suggested that CK-mediated resistance functions through salicylic acid (SA)

16   dependent mechanisms (Choi *et al.*, 2010). An additional study suggested that CK signaling

17   enhances the contribution of SA-mediated immunity in hormone disease networks (Naseem *et*

18   *al.*, 2012). However, in tobacco, an SA-Independent, phytoalexin-dependent mechanism was

19   suggested (Grosskinsky *et al.*, 2011). We recently reported that CK induces systemic immunity

20   in tomato (*Solanum lycopersicum*), promoting resistance to fungal and bacterial pathogens

21   (Gupta *et al.*, 2020a,b) including *Botrytis cinerea,* in an SA and ethylene dependent mechanism.

22   *B. cinerea* (grey mold), *Sclerotium rolfsii* (collar rot), and *Fusarium oxysporum* f. sp. *lycopersici*

23   (fusarium wilt) are widespread fungal plant pathogens that infect hundreds of plant species and

3

24   cause huge losses every year (Tsahouridou & Thanassoulopoulos, 2002; Williamson *et al.*, 2007;

25   Dean *et al.*, 2012).

26   Given that CK can induce plant immunity and restrict phytopathogen growth in certain cases,

27   direct effects of CK against phytopathogens are an intriguing possibility. A direct effect of CK

28   on bacterial pathogens was ruled out in previous works (Naseem *et al.*, 2012; Gupta *et al.*, 2020a).

29   Interestingly, CK did not affect germination and elongation of germ tubes, but strongly inhibited

30   appressorium formation of *Erysiphe graminis*, an obligate biotrophic powdery mildew causing

31   barley pathogen (Liu & Bushnell, 1986). Another work described an increase in germination of

32   conidia of two *Erysiphe* powdery mildew pathogens, *E. graminis* and *E. cichoracearum*, in the

33   presence of CK (Mishina *et al.*, 2002). Fungal pathogens of the species *Erysiphe* are known to

34   produce CKs. High levels of CK was also reported to inhibit mycelial growth and pathogenesis

35   of fungi in canola (Sharma *et al.*, 2010).

36   In this work, we investigate the direct effects of CK on fungal plant pathogens, demonstrating

37   that CK directly inhibits the growth, development, and virulence of fungal plant pathogens. *B.*

38   *cinerea* (*Bc*) growth, sporulation, and spore germination were all inhibited by CK, in the absence

39   of a host plant. We found similar effects in a variety of plant pathogenic fungi. Molecular and

40   cellular analyses revealed that CK is not toxic to *Bc*, but rather, *Bc* likely recognizes CK and

41   responds to it, resulting in cell cycle and individual cell growth retardation. CK reduced *Bc*

42   virulence in a reversible manner, confirming that no irreversible harm was caused to fungal

43   development. RNAseq confirmed that CK downregulates the cell cycle and cytoskeleton, as well

44   as cellular trafficking. Interestingly, we also found that CK affects two additional fungi from the

45   ascomycota division that are not phytopathogens, but rather, yeasts. Both budding and fission

46   yeast were inhibited by CK. Further to the effects observed in the RNAseq data, we confirmed

47   that CK affects the cytoskeleton and cellular trafficking in *Bc*, mislocalizing actin filaments and

48   lowering endocytic rates and endomembrane compartment sizes, likely underlying the reduced

4

49   growth rates and arrested developmental programs. Mutant analyses in yeast confirmed that the

50   endocytic pathway is affected by CK. Our work uncovers a novel, remarkably conserved role for

51   a primary plant growth hormone in fungal biology, demonstrating that interaction between

52   pathogen and host resulted in fascinating molecular adaptations on fundamental processes in

53   eukaryotic biology. In time, this may hold promise for the development of CKs as antifungal

54   agents in specific cases.

55

56   **Results**

57   **Cytokinin inhibits disease caused by *B. cinerea* and *S. rolfsii*, but not *F. oxysporum* f. sp.**

58   *lycopersici*

59   We have previously reported that CK reduces tomato disease by inducing immunity (Gupta *et*

60   *al.*, 2020b). Fungal pathogens with different lifestyles have different infection and pathogenesis

61   strategies, and host plants employ different protection mechanisms to resist different types of

62   fungal pathogens. Three phytopathogenic fungi with varied lifestyles and infection modes were

63   selected. *B. cinerea (Bc),* an airborne necrotrophic spore producing ascomycete, that causes gray

64   mold disease in >1400 hosts (Fillinger & Elad, 2016); *S. rolfsii (Sr)-* a soilborne necrotrophic

65   basidiomycete that does not produce spores, that causes southern blight disease in hundreds of

66   hosts (Arnold, 2008); and *F. oxysporum* f. sp. *lycopersici (Fol)*, a soilborne necrotrophic

67   ascomycete that is known to produce CK (Vrabka *et al.*, 2018; Sørensen *et al.*, 2018), and causes

68   wilt disease in a host specific manner (Stravato *et al.*, 1999). In order to examine the ability of

69   CK to reduce disease caused by different fungal pathogens, we treated tomato plants with 100

70   μM CK (6-BAP) 24 hours prior to pathogen inoculation. **Fig. 1** details the effect of CK in tomato

71   disease caused by different phytopathogens. 6-BAP pre-treatment significantly decreased disease

72   levels caused by the necrotrophic fungal pathogens *Bc* , as we previously reported (Gupta *et al.*,

73   2020b) (**Fig. 1a**), and *Sr* (**Fig. 1b**). Upwards of 50% disease reduction in tomato plants was

74   observed with *Bc* and *Sr* as compared to control (**Fig. 1 a,b**). However, no disease reduction was

75   observed with *Fol* (**Fig. 1c**).

76   **Cytokinin directly inhibits *B. cinerea*, *S. rolfsii*, and *F. oxysporum* f. sp. *lycopersici***

77   In order to examine a possible direct effect of CK on fungal tomato pathogens, we used the above

78   three phytopathogenic fungi. The effects of different CK concentrations and derivatives on the

79   growth of *Bc, Sr* and *Fol* mycelia are shown in **Fig. 1**. The cyclic synthetic CK 6-BAP (**Fig. 1d-**

80   **k**), the natural cyclic CKs zeatin and kinetin (**Fig. 1k**), and the synthetic bacterial derived non-

81   cyclic CK thidiazurn (TDZ, **Fig. 1k**)- all inhibited the growth of *B. cinerea*. 6-BAP (6-benzyl

82   amino purine) inhibited the growth of *Bc* in a dose-dependent manner. Approximately 50%

83   inhibition was observed at 100 µM (**Fig. S1a**). *Sr* did not show growth reduction at 1 µM but

84   growth inhibition at 10 µM and 100 µM was similar to *Bc* (**Fig. S1b**). The least effect of 6-BAP

85   was observed on *Fol* (**Fig. S1c**), which was not inhibited by CK treatment *in planta* (**Fig. 1c**).

86   To examine the breadth of this phenomenon, we tested *in vitro* growth of additional

87   phytopathogenic fungi in the presence of 100 µM 6-BAP or the control Adenine. Our results

88   show that CK directly inhibits mycelial growth of fungal pathogens from several different classes

89   (ascomycetes, basidiomycetes) and different lifestyles (hemibiotrophs, necrotrophs) (**Fig. S2**).

90   All classes of phytopathogenic fungi tested were inhibited by CK (**Fig. S2a**), however, the level

91   of inhibition also differed significantly among them, with *Fusarium* spp. showing the least

92   inhibition (**Fig. S2b**). The phylogeny is detailed in **Fig. S2c**, and does not indicate that the ability

93   to be inhibited by CK is specific to any particular class or taxon.

94   **Cytokinin inhibits *B. cinerea* sporulation, spore germination, and germ tube elongation**

95   We studied the effect of CK fungal development: sporulation, spore germination, and germ tube

96   elongation. In samples treated with 100 nM CK, there were approximately 50% less spores

6

97 produced as compared to mock (**Fig. 2a,b**). The effect of CK on spore germination was even

98 more pronounced (**Fig. 2c,d**). Less than 50% of the spores germinated with 100 nM CK.

99 Interestingly, though less spores germinated in the presence of 6-BAP, the spores that did

100 germinate had accelerated germ tube growth in 100 nM 6-BAP, and inhibited germ tube growth

101 100 µM 6-BAP (**Fig. 2c,e**). After 8 hours of growth with 100 µM 6-BAP, the germ tube length

102 was 50% of the control (**Fig. 2e**), correlating with ~50% inhibition in mycelial growth (**Fig.**

103 **1d,e,j,k**).

104 LC/MS Hormonal measurements in mature tomato leaves demonstrate that they can contain close

105 to 100 ng/g active CKs (**Fig. S3**), as was previously reported for tomato leaves (Ghanem *et al.*,

106 2008; Žižková *et al.*, 2015). This amount roughly corresponds, depending on the CK derivative,

107 to 400-500 nM, which did not affect mycelial growth of the phytopathogenic fungi we tested

108 (**Fig. S1**), but did inhibit sporulation and spore germination in *B. cinerea* (**Fig. 2b-d**).

109 **Cytokinin reversibly attenuates *B. cinerea* virulence**

110 Is direct CK inhibition of phytopathogenic fungi reversible? Or does CK irreversibly harm fungal

111 development? Furthermore, since some aspects of *Bc* development are inhibited in CK

112 concentrations normally found within plant leaves (**Figs. 2, S3**), how does CK affect fungal

113 virulence? To answer these questions, we harvested *Bc* spores from fungi grown with or without

114 CK, normalized the spore count to 10^5 spores/mL, and used equal amounts of spores to infect

115 tomato leaves. When spores harvested from mycelia grown with 6-BAP were used for infecting

116 tomato leaves, no reduction in lesion size was observed as compared with spores grown without

117 CK (**Fig. 3a**). We harvested spores from mycelia grown without CK, mixing half the spores with

118 CK just prior to tomato leaf infection. When spores were treated with CK prior to infection, there

119 was approximately 40% reduction in lesion area (**Fig. 3b**), comparable to disease reduction

120 observed when treating plants with CK (**Fig. 1a**).

121 CK differentially down-regulated the expression levels of virulence genes in *Bc* (**Fig. 3c**). All

122 tested genes related to virulence viz., *BcPG1* (endopolygalacturonase)*, BcXynl, BcXyn10A* and

123 *BcXyn11C* (Xylanases)*, BcPME1* (pectin methylesterase)*, BcPLC1* (phospholipase C)*, BcBMP1*

124 (mitogen-activated protein (MAP) kinase) and *BcPLS1* (tetraspanin) were expressed at

125 significantly lower levels upon growth in the presence of 100 µM of 6-BAP. In addition, the

126 expression of the woronin body protein *Bchex*, known to be involved in fungal membrane

127 integrity (Torres-Ossandón *et al.*, 2019), was down-regulated upon CK treatment. . Gene

128 expression was normalized to a geometric mean of 3 housekeeping genes: ubiquitin-conjugating

129 enzyme E2 (*ubce*) (Silva-Moreno *et al.*, 2016), Iron-transport multicopper oxidase, and

130 Adenosine deaminase (Llanos *et al.*, 2015).

131

132 **Cytokinin is not toxic to *B. cinerea***

133 Why is CK inhibiting fungal growth and development? Spores generated from fungus grown in

134 the presence of CK were able to infect tomato leaves normally, once removed from the CK

135 containing environment, indicating that the spores themselves were normal, and that disease

136 reduction stems from a reduction in spore formation, spore germination, and germ tube growth

137 (**Fig. 3**). To confirm that CK is not killing fungal cells, we examined fungal cellular leakage in

138 the presence of CK. As shown in **Fig. 4a,b**, no significant leakage of nucleic acids and proteins

139 were observed after 24 h treatment with 100 µM 6-BAP, when compared to the control.

140 Additionally, no change in electrical conductivity was observed upon 24 hours of 100 µM 6-

141 BAP treatment (**Fig. 4c**). The high background measurements with CK alone are likely due to

142 the presence of the aromatic ring structure. These results confirm that CK is not toxic to *Bc*.

143 **Transcriptome profiling reveals pathways affected by CK in *B. cinerea***

144 To gain insight into the effects CK has on the fungus, we conducted transcriptome profiling on

145 *Bc* samples prepared from fungi grown with and without CK. Principle component analysis

146 demonstrated that the biological replicates were clustered well together (**Fig. 5a**), with mock

147 samples being very similar, and CK samples clustering together across PC1 (75%). The

148 comparison yielded two clusters, exemplified in a heatmap (**Fig. 5b**): genes downregulated by

149 CK when compared with mock (bottom cluster, marked in red) and genes upregulated by CK

150 when compared with mock (top cluster, marked in green). Individual genes having a $\log_{(2)}$Fold-

151 change of |2| or greater are provided in **Supplementary Data 1**. Interestingly, out of the 660

152 differentially expressed genes (DEGs), 470 were down regulated, indicating that CK has more

153 of a suppressive effect on the *Bc* transcriptome. Distribution of DEGs into various biological

154 pathways in Kyoto Encyclopedia of Genes and Genomes (KEGG) also supports this.

155 Downregulated KEGG pathways included various pathways related to the cell cycle and DNA

156 replication (**Fig. 5c**), as well as endocytosis, MAPK signaling, and a variety of metabolic

157 pathways (**Fig. 5c**). The full KEGG list with adjusted p-values for each pathway is provided in

158 **Supplementary data 2**. Upregulated KEGG pathways included various pathways related to

159 protein biosynthesis and processing (**Fig. 5d**), as well as the peroxisome and phagosome (**Fig.**

160 **5d**). The full KEGG list with adjusted p-values for each pathway is provided in **Supplementary**

161 **data 3**.

162

163 **Cytokinin affects the fungal cell cycle**

164 Since we observed that CK inhibits sporulation, spore germination, and hyphal growth, and the

165 cell cycle and DNA replication were down regulated by CK treatment in the transcriptome

166 analysis, we examined the morphology and relative DNA quantity of *Bc* cells grown with and

167 without CK (**Fig. 6**). We observed a significant reduction of ~75% in cell size upon CK treatment,

168   with cells also appearing rounder (**Fig. 6a,b,d**).The distance between the last two septa from the

169   hyphal tip were reduced to about 30% of normal length (**Fig. 6e**). 8 hours after germination, CK

170   grown hyphae produced less than half the number of septa when compared with mock grown

171   hyphae (**Fig. 6f**), further confirming that cell replication is inhibited. Concurrently, we quantified

172   Hoechst staining in mock and CK grown mycelia. Hoechst binds to DNA and has been used

173   before to estimate DNA content in live cell nuclei (Gomes *et al.*, 2018). CK grown cells were

174   stained by Hoechst less than 50% of the amount of stain observed in mock grown cells (**Fig.**

175   **6c,g**). Images were taken under identical conditions. Reduction in Hoechst staining coupled with

176   lower rates of cell replication and the transcriptomic data indicating downregulation of cell cycle

177   and meiosis pathways, indicates that CK may be inhibiting mitosis in *Bc*.

178

179   **Cytokinin inhibits the fungal cytoskeleton**

180   Our results demonstrate that CK inhibits fungal growth and development (**Figs. 1,2,5**). We

181   hypothesized that CK affects a fundamental cellular process relevant to most fungi; a process

182   that is crucial to execute the fast growth occurring in hyphal tips (Bartnicki-Garcia, 2002), growth

183   that requires membrane remodeling (Riquelme *et al.*, 2018). Based on the NGS results, we

184   hypothesized that these affected processes, in addition to the cell cycle, are likely to be

185   cytoskeletal integrity and/or cellular trafficking.

186   To examine cytoskeleton integrity, we first validated the expression levels of cytoskeletal genes

187   shown to be differential in the transcriptomic data. These genes are listed in **Fig. 7a** (saturated

188   blue color indicates downregulation), with the full expression data provided in **Supplementary**

189   **Data 4**. We independently confirmed relative expression of 5 genes from the data set by qRT-

190   PCR, selecting both down regulated and up-regulated genes from the transcriptome (**Fig.7b**). As

191   such, we used the geometric mean of 3 housekeeping genes that are unrelated to the cytoskeleton

10

192   for gene expression normalization. We transformed *B. cinerea* with the filamentous actin marker

193   lifeactin-GFP (Schumacher, 2012), and proceeded to treat the transformed fungal cells with CK.

194   We observed mislocalization of life-actin, which is normally localized to growing hyphal tips

195   (Walker & Garrill; Berepiki *et al.*, 2011), upon CK treatment. CK caused life-actin to be

196   distributed more uniformly throughout the cells, and to lose most of its tip-specific localization

197   (**Fig. 7c-d**). Analysis of corrected total fluorescence in mock and CK treated cells demonstrated

198   that the ratio between life-actin in the tip of the cell, and the total cell, decreased greatly in the

199   presence of CK (**Fig. 7d**). Note that the transformed fungus showed the characteristic "split tips"

200   phenotype of lifeactin overexpression (Schumacher, 2012) in both mock and CK treated samples.

201

Cytokinin inhibits fungal endocytosis

203   We and others (Marhavý *et al.*, 2011; Gupta *et al.*, 2020b) have previously shown that CK can

204   influence cellular trafficking in plants. Further to our results demonstrating that CK inhibits the

205   cytoskeleton in *B*c, and since the endocytic pathway was also found to be significantly

206   downregulated by CK (**Fig. 5**), we examined the effect of CK on endocytosis in *Bc*. **Fig. 8** shows

207   that 6-BAP inhibits endocytosis of the endocytic tracer FM-4-64, which is routinely used in fungi

208   (Fischer-Parton *et al.*, 2000), reducing the amount of endocytic vesicles by more than 50% (**Fig.**

209   **8a,b**). 6-BAP also caused a significant decrease in the size of the vesicles containing endocytic

210   tracer (**Fig. 8c**), in both the 100 nM and 100 uM concentrations, similar to its effect on sporulation

211   and spore germination (**Fig. 2**). This suggests that in parallel with the effect on the cytoskeleton,

212   CK has a possible impact on membrane function and/ or fission of vesicles.

Inhibition of endocytosis abolishes *B. cinerea* CK sensitivity

214   To further examine the effect of CK on endocytosis inhibition in *Bc*, we examined combined

215   effects of CK and endocytosis inhibition using butanol treatments. 1-butanol inhibits

11

216   phospolipases (Motes *et al.*, 2005; Jia & Li, 2018), which have been linked to both growth and

217   virulence in *Bc* (Schumacher *et al.*, 2008) (see also **Fig. 3**), and was used as an endocytosis

218   inhibitor in previous works in fungi (Boucrot *et al.*, 2006; Sharfman *et al.*, 2011; Li *et al.*, 2012).

219   We examined CK-mediated growth inhibition of both mycelia area and dry weight, in the

220   presence or absence of the endocytosis inhibitor 1-butanol, as well as its structural analog 2-

221   butanol, which does not inhibit endocytosis (Sharfman *et al.*, 2011). **Fig. S4** demonstrates that

222   upon endocytosis inhibition with 1-butanol, CK no longer affects fungal growth, while CK-

223   mediated growth inhibition is retained in the mock and 2-butanol treatments. (**Fig. S4 a,b**). At

224   0.4%, 2-butanol did not inhibit fungal growth. At 0.8%, fungal growth inhibition was observed

225   with 2-butanol, though to a significantly lesser degree than that observed with 1-butanol (**Fig.

226   S4a**).

227   Inhibition of the cytoskeleton abolishes *B. cinerea* CK sensitivity

228   We further examined combined effects of CK and cytoskeleton disruption, using Benomyl (Ben)

229   and Latrucnculin B (LatB). Benomyl depolymerizes microtubules, and has been previously used

230   as a fungicide, and in studies of fungal cell cycle and cytoskeleton (Momany & Hamer, 1997;

231   Peterson & Mitchison, 2002; Dub *et al.*, 2013). Latrunculin B depolymerizes actin filaments, and

232   has also previously been used for cytoskeletal studies in fungi (Ketelaar *et al.*, 2012). We assayed

233   the combined effect of CK and Ben or LatB on endocytosis, assaying endosome size and density.

234   We observed that CK and Ben (**Fig. S5a,c**) or LatB (**Fig. S5b,d**) affect endocytic compartments

235   in a similar manner, finding no enhancement of endocytosis inhibition when CK was combined

236   with either drug (**Fig. S5**), suggesting that CK may inhibit endocytosis in part through its effect

237   on the cytoskeleton, though down regulation of endocytic genes is also present (**Fig. 5**).

238   We also examined the combined effect of CK and Ben or LatB on growth inhibition of fungal

239   mycelia. **Fig. S6** demonstrates that Ben and LatB mediated growth inhibition is not further

240   enhanced by the addition of CK. Pursuant to the results presented in Figure 5, the size of hyphal

241   cells treated with CK, Ben (**Fig. S6a**), LatB (**Fig. S6b**), or combinations of Ben/LatB and CK,

242   was similarly reduced when compared with mock treated cells, demonstrating that CK may have

243   a similar effect as Ben or LatB on the progression of the cell cycle. Additionally, colony mycelial

244   area, which was reduced by Ben and LatB in a concentration dependent manner, remained mostly

245   unaffected by the addition of CK in the background of these drugs (**Fig. S6c,d**).

246

247   **Cytokinin reduces yeast growth and endocytosis**

248   Given our observations that CK can affect fundamental cellular processes in fungi, we examined

249   inhibitory roles for CK in the growth of *Saccharomyces cerevisiae*, a budding yeast, and

250   *Schizosaccharomyces pombe*, a fission yeast, the growth of which more closely resembles that

251   of fungal hyphae. Growth curves were generated by measuring OD_{600} over time, as previously

252   described (Laor *et al.*, 2019). We observed that CK inhibits the growth of *S. cerevisiae* (**Fig.**

253   **9a,b**)*,* and *S. pombe* (**Fig. S7a,b**) in a dose-dependent manner. We found that *S. pombe* was more

254   strongly inhibited. Interestingly, trans zeatin was previously reported not to affect *S. pombe* cell

255   division (Suzuki *et al.*, 2001).

256   To examine whether growth inhibition is mediated by endocytosis in yeast, as we found for *Bc*,

257   we conducted endocytic assays in *S. cerevisiae* (**Fig. 9**) and *S. pombe* (**Fig. S8**). Yeast cultures

258   were grown overnight, diluted to an OD_{600} of 0.2, and grown for a further six hours with or

259   without CK. Cultures were then stained with FM4-64 (Vásquez-Soto *et al.*, 2015). CK reduces

260   cell size, internalization of FM4-64, endosome size, and endosome density in both *S. cerevisiae*

261   (**Fig. 9c-f**) and *S. pombe* (**Fig. S8a-e**

262   In parallel, the effect of CK on the growth of *S. cerevisiae* endocytic mutants was examined.

263   Genes known to be involved in endocytosis, the absence of which is known not to be lethal, were

13

264   selected. *S. cerevisiae* knockout strains were generated as described in the methods section.

265   Mutations in *YPT31*, a Rab/GTPase known to be involved in vesicular trafficking (Jedd *et al.*,

266   1997), *SSA1*, known to be involved in clathrin vesicle uncoating (Krantz *et al.*, 2013), *VPS1*, a

267   dynamin-like GTPase known to be required for vacuolar sorting, cytoskeleton organization and

268   endocytosis (Vater *et al.*, 1992; Ekena *et al.*, 1993) and *SPO14*, a phospholipase D protein

269   required for sporulation (Rudge *et al.*, 2002), were generated and examined. Three out of the four

270   generated mutants, *ypt31Δ*, *ssa1Δ*, and *vps1Δ*, exhibited a partial rescue in CK mediated

271   inhibition (**Fig. 10a-c,e,f**), growing significantly better in the presence of 300 and 500 μM 6-

272   BAP than the wild type (WT) strain. The *spo14Δ* mutation did not rescue CK-mediated growth

273   inhibition (**Fig. 10d-f).**

274

275   **Discussion**

276   As reported previously by us and others, and as shown here (**Fig. 1**), CK promotes fungal disease

277   resistance in plants (Choi *et al.*, 2010; Gupta *et al.*, 2020b). Direct effects of CK on fungal growth

278   and development have not been investigated in depth in plant-free systems, and although a few

279   studies have discussed some effects of CK on fungal pathogen growth (Babosha, 2009; Sharma

280   *et al.*, 2010), no mechanisms for CK antifungal activity have yet been reported. The present study

281   was performed to examine the direct inhibitory effect of CK on different classes of fungal

282   phytopathogens. We focused our efforts on three pathogens, *Bc, Sr* and *Fol*, with varied lifestyles

283   and infection modes.

284   We found that CK treatment strongly inhibits *Bc* and *Sr*, and inhibits *Fol* more weakly (**Fig. 1d-**

285   **j**). It has been demonstrated that pathogenic fungi of the *Fusarium* species complex are able to

286   produce CKs endogenously, which might be the reason for its tolerance towards exogenous CK

287   (Vrabka *et al.*, 2018; Sørensen *et al.*, 2018). Interestingly, varying levels of inhibitory activity

288   were observed for CK in many phytopathogenic fungi (**Fig. S2**).

289   Examination of possible effects of CK on *Bc* development revealed that CK attenuates *Botrytis*

290   sporulation, spore germination and germ tube elongation (**Fig. 2**), with differential effects of the

291   CK concentration on different processes. Interestingly, genes involved in the regulation of

292   growth, conidiation, germination, virulence, and pathogenicity in *Bc*, were strongly inhibited by

293   CK treatment (**Fig. 3**). Several genes previously found to be involved in plant infection processes

294   and defined as essential determinants for *Bc* pathogenicity (Zheng *et al.*, 2000; Valette-Collet *et*

295   *al.*, 2003; Gourgues *et al.*, 2004; Brito *et al.*, 2006; Schumacher *et al.*, 2008; Aguayo *et al.*, 2011;

296   Frías *et al.*, 2019) were found to be significantly downregulated upon CK treatment (Figure 3c).

297   This suggests that interference with the expression of virulence genes may also partly contribute

298   to the inhibitory effects of CK against *Bc*. Inhibition of growth and spore germination together

15

299   with downregulation of virulence genes in *Bc* could account for plant disease attenuation. This

300   mechanism could complement the plant induced resistance mechanisms being activated by CK,

301   which, as reported by us and others (Choi *et al.*, 2010; Argueso *et al.*, 2012; Gupta *et al.*, 2020b),

302   induces plant immunity even in the absence of a pathogen.

303   Damage in cell membrane integrity in fungi usually leads to the release of nucleic acids and

304   proteins (Lewis & Papavizas, 1987; Ji *et al.*, 2018; Wang *et al.*, 2020). CK showed no effect on

305   leakage of nucleic acids and proteins from *Bc* after treatment, and no change was observed in

306   media conductivity of *Bc* after CK treatment, indicating that cell membrane permeability

307   remained unchanged. Taken together, these results suggest that CK is not toxic to fungi. CK can

308   thus be defined as possessing fungistatic, and not fungicidal, activity.

309   To understand the mode of action by which CK inhibited the growth of *Bc*, we conducted

310   transcriptome profiling on *Bc* with and without CK. RNAseq data suggested that CK

311   downregulates the cell cycle and cellular cytoskeleton and trafficking processes in *Bc*. Thus, we

312   examined cell morphology and DNA replication after CK application. CK strongly reduced cell

313   area, distance between septa, and likely, mitosis (**Fig. 6**). Cell division/septum formation is

314   dependent on the signals generated during cell extension and growth, and nuclear division.

315   Reduced cell growth and elongation effected by CK treatment correlates with the lesser number

316   of septa in the treated cells. Hoechst staining revealed there is less DNA in CK treated cells,

317   possibly due to inhibition of mitosis. Benomyl treatment, which is known to arrest the cell cycle,

318   caused decreases in cell sizes that were not further augmented by CK (**Fig. S6**). Taken together,

319   inhibition of cell division (septa formation) coupled with reduced DNA amounts and activity

320   similar to benomyl, strongly support the notion that CK is inhibiting mitosis in fungal cells.

321   Also evident from the transcriptomic data was the effect of CK on the cytoskeleton and endocytic

322   processes. Indeed, we found that CK caused mislocalization of actin at the growing tip of hyphae

16

323   (**Fig. 7**), likely explaining, at least in part, the reduced hyphal growth observed (**Fig. 1**). CK

324   inhibited the amount of endocytic vesicles in *Bc* (**Fig. 8**), *S. cerevisiae* (**Fig. 9**), and *S. pombe*

325   (**Fig. S8**), indicating that it likely has an impact on membrane function and/ or fission of vesicles.

326   Cell elongation, in particular hyphal elongation, requires continuous addition of new plasma

327   membrane, proteins, and cell wall material at the hyphal tip. Cellular trafficking and

328   endo/exocytosis, which depen both on an intact cytoskeleton and on endocytic compartments,

329   regulate the amount of membrane transferred towards this cellular growth, tightly controlling the

330   amount of cellular material required for plasma membrane extension (Riquelme *et al.*, 2018).

331   Inhibition of the cytoskeleton and endocytosis by CK explains the reduced elongation and growth

332   of *Bc* and yeast cells. Fission yeast may be more reliant on cellular trafficking for rapid cell

333   elongation than budding yeast, and their growth is more similar to the growth of fungi than that

334   of budding yeasts, possibly also explaining why fission yeast was more strongly inhibited by CK

335   than budding yeast.

336   It has been previously suggested that certain classes of fungi possess CK receptors to be able to

337   "sense plants", a trait posited to have been required for land colonization by fungi (Hérivaux *et*

338   *al.*, 2017). We and others have previously demonstrated that plants activate CK signaling upon

339   pathogen attack, and that CK serves as a cue to activate defense responses (Choi *et al.*, 2010;

340   Argueso *et al.*, 2012; Gupta *et al.*, 2020b). A possibility arising from our work is that when plants

341   sense the presence of phytopathogenic fungi, an additional reason for the activation of CK

342   pathways is to promote CK biosynthesis, thereby inhibiting the growth of the potential fungal

343   attacker. We have shown here that CK inhibits growth in different types of fungi from different

344   classes (basidiomycetes, ascomycetes) and lifestyles (soilborne, airborne, hemibiotroph,

345   necrotroph), and yeasts (**Figs. 1, 2, 5, 8, S1, S2**), and cellular trafficking in *Bc*, *S. cerevisiae*, and

346   *S. pombe* (**Figs. 6, 7, 9, S3**). Chemically or genetically attenuating cellular trafficking in *Bc* (**Fig.**

347   **7**), or *S. cerevisiae* (**Fig. 10**) respectively, resulted in loss of CK mediated growth inhibition. It

17

348   would seem that, in employing CK as a fungal pathogen inhibitor, plants have succeeded in

349   managing to target processes fundamental to growth, such that this inhibition is preserved all the

350   way to budding yeast.

351

352   In the evolutionary war against plant pathogens, plants appear to have succeeded in creating a 1-

353   2 mechanism for utilization of CK, previously believed to be only a "developmental" hormone.

354   1- The plant senses a pathogen and activates its CK response, leading to immunity signaling,

355   which culminates in increased immunity and systemic pathogen resistance; and 2- the activation

356   of CK response leads to the generation of increased CK levels, which inhibit the growth and

357   development of fungal pathogens by targeting their cell cycle and trafficking machinery. Future

358   work will validate the genetic targets of CK in fungi, and whether this fungistatic activity can be

359   agriculturally adapted.

360

Materials and Methods

Pathogen growth conditions

Botrytis cinerea (strain Bcl16), *Sclerotium rolfsii* (Liarzi *et al.*, 2020), *Fusarium oxysporum* f. sp. *lycopersici* (strain 4287) were cultivated on potato dextrose agar (PDA) at $22 \pm 2\,°C$ for *B. cinerea*, $26 \pm 2\,°C$ for *S. rolfsii* and $28 \pm 2\,°C$ for *F. oxysporum* for 5-7 days. Pathogen isolates were kindly gifted by Yigal Elad, David Ezra and Shay Covo.

Chemical treatments

6-BAP (6-Benzylaminopurine), zeatin, kinetin, TDZ, (all in 10mM NaOH), adenine (1M HCL), Benomyl and latrunculinB (DMSO), 1-butanol and 2-butanol, were all obtained from Sigma-Aldrich, and added to media at indicated concentrations.

Cytokinin level measurement

Cytokinin extraction was performed according to (Gupta *et al.*, 2020b). Solvent gradients and MS-MS parameters are detailed in supplemental Table 1.

Plant pathogenesis assays

Bc pathogenesis was performed as previously described (Gupta *et al.*, 2020b).

Fol culture was grown in KNO_3 media (yeast nitrogen base, sucrose, KNO_3 and distilled water) at $28\,°C$ for 5 days. . Two week old tomato plants were treated with $100\,\mu M$ 6-BAP (foliar spray) and inoculated with a spore suspension (10^6 spores ml^{-1}) (De Cal *et al.*, 2000) using the root dip method (Wellman, 1939; Mes *et al.*, 1999), 24 h later. The disease index (DI) was calculated after three weeks of using a 0–5 scale: 0, no symptoms; 1, $\leq 2\%$ (healthy plant); 2, 3–30% (slight disease); 3, 31–60% (moderate disease); 4, 61–90% (severe disease), and 5, $\geq 91\%$ (dead plant). For *Sr*, tomato plants were soil drenched with $100\,\mu M$ of 6-BAP or mock (NaOH + Tween 20) one week prior to infection. After one week, 3-4 sclerotia of *Sr* were placed on the soil, ~2cm from the plant stem. DI was assessed after 2 weeks.

385 *B. cinerea* **spore germination measurement**

386 *B. cinerea* spores (10^6 spores ml^{-1}) were incubated in potato dextrose broth (PDB) containing 0

387 and 100 µM 6-BAP at 22 ± 2 °C for 8 hours. Conidia were washed twice in sterile water (1 ml),

388 centrifuged at 12,000 rpm for 5 min, and re-suspended in 100 µL of sterile water. A 10 µL sample

389 was analyzed under the microscope. The percentage of sporulation, spore germination and the

390 length of germ tubes were measured using ImageJ software.

391 **Measurement of cellular leakage and electrolytes**

392 *Bc* were treated with 6-BAP (0 and 100 µM) in PDB and incubated on a rotary shaker at 180 rpm

393 for 24h at 22 °C. The mycelia were subsequently centrifuged and the aqueous solutions were

394 used for measurement of the leakage of nucleic acids and proteins. The absorbance of the

395 supernatant was measured at 595 nm using UV/VIS spectrophotometer. Leakage of proteins was

396 quantified according to Bradford (Bradford, 1976). The release of nucleic acids in various

397 treatments was measured by detecting the optical density at 260 nm. Electrical conductivity was

398 measured using a conductivity meter (EUTECH instrument con510) after 24 h.

399 *B. cinerea* **qRT-PCR virulence assessment**

400 *Bc* spores were grown in PDB with 0 and 100 µM 6-BAP in a rotary shaker at 180 rpm and 22 ±

401 2 ℃ for 24 hours. RNA was isolated using Tri-reagent (Sigma-Aldrich) according to the

402 manufacturer's instructions. cDNA was prepared and qRT-PCR was performed as previously

403 described (Gupta *et al.*, 2020b). The primer sequences for each gene, and primer pair efficiencies,

404 are detailed in Supplementary Table 2. A geometric mean of the expression values of the three

405 housekeeping genes*:* ubiquitin-conjugating enzyme E2 (ubce) (Silva-Moreno *et al.*, 2016), Iron-

406 transport multicopper oxidase, and Adenosine deaminase (Llanos *et al.*, 2015) was used for

407 normalization of gene expression levels. Relative gene expression levels were calculated using

408 the $2^{-\Delta\Delta Ct}$ method (Pfaffl, 2001).

RNA extraction, quality control and RNA-sequencing

410   Total RNA was extracted from liquid *B. cinerea* cultures grown for two days in 1/2 PDB with

411   the addition of tobacco seedlings 5 days post germination (150 seedlings/ 50 mL media), mock

412   or supplemented with 25uM 6BAP, 50 mg fungal mass per sample, using the Norgen total RNA

413   purification kit (Norgen Biotek corp.) according to the manufacturer's instructions. RNA yield

414   and purity was measured by Nanodrop (ND-1000 Spectrophotometer, Wilmington, USA), and

415   validated by Bioanalyzer 2200 TapeStation (Agilent Technologies, California, USA). cDNA

416   libraries with multiplexing barcodes were prepared using the TrueSeq RNA kit (Illumina, San

417   Diego, CA, USA). Libraries were evaluated with Qbit and TapeStation (Agilent Technologies,

418   California, USA). Pooled libraries of the 6 samples were sequenced on one lane of an Illumina

419   Hiseq 2500 instrument using a 60-bp single-end RNA-Seq protocol, to obtain ~20 million reads

420   per sample. Sequencing was performed at the Weizmann Institute of Science, Israel.

421   **Transcriptome analysis**

422   Raw-reads were subjected to a filtering and cleaning procedure. The Trimmomatic tool was used

423   to filter out adapter sequences, remove low quality sequences by scanning a 4-base wide sliding

424   window, cutting when the average quality per base drops below <15 and finally, removal of reads

425   shorter than 36 bases (Bolger *et al.*, 2014). Clean reads were mapped to the reference genomes

426   of *B. cinerea* B05.10 (assembly accession GCF_000143535.2) (Staats & van Kan, 2012) using

427   STAR software (Dobin *et al.*, 2013). Gene abundance estimation was performed using Cufflinks

428   version 2.2 (Trapnell *et al.*, 2012) combined with gene annotations from genbank. Heatmap

429   visualization was performed using R Bioconductor (Gentleman *et al.*, 2004). Gene expression

430   values were computed as FPKM. Differential expression analysis was completed using the

431   DESeq2 R package (Love *et al.*, 2014). Genes with an adjusted p-value of no more than 0.05 and

432   log2FC greater than 1 or lesser than -1 were considered differentially expressed. PCA was

21

433   calculated using the R function prcomp. We submitted the raw sequencing data generated in this

434   study to NCBI under bioproject accession number PRJNA718329.

435   The gene sequences were used as a query term for a search of the NCBI non-redundant (nr)

436   protein database that was carried out with the DIAMOND program (Buchfink *et al.*, 2014). The

437   search results were imported into Blast2GO version 4.0 (Conesa *et al.*, 2005) for gene ontology

438   (GO) assignments. Gene ontology enrichment analysis was carried out using Blast2GO program

439   based on Fisher's Exact Test with multiple testing correction of false discovery rate (FDR).

440   KOBAS 3.0 tool (http://kobas.cbi.pku.edu.cn/kobas3/?t=1) (Xie *et al.*, 2011) was used to detect

441   the statistical enrichment of differential expression genes in KEGG pathway and Gene Ontology

442   (GO).

443   **Cell elongation and DNA content**

444   *Bc* spores were cultured in PDB with or without 6-BAP (100 µM) at 22 °C for 8 (septa counting

445   in individual hyphae) or 16 h. The cells were then collected and stained with 1 g l^{-1} calcofluor

446   white M2R at room temperature for 15 min, or 15 ug ml^{-1} Hoechst 33342 (Sigma-Aldrich) in the

447   dark for 1 h in a humid chamber at room temperature (Dub *et al.*, 2013).

448   Nuclei and septa were visualized with an Olympus 398 IX 81 confocal microscope (Fluoview

449   500) equipped with a 60× 1.0 NA PlanApo water immersion objective. Images were acquired

450   using a 399 nm excitation laser (1% power), with emission collected in the range 385-420 nm.

451   Images were analyzed using Fiji-ImageJ. Cell size and length (septal distance) were measured

452   using the area measurement tool. Septa were counted using the counter tool. DNA staining was

453   assessed using mean intensity measurement.

454   ***B. cinerea* transformation**

455   We used the plasmid pNDH-OLGG (Schumacher, 2012) to generate *B. cinerea* expressing

456   lifeact-GFP. The transformation cassette was amplified using primers GA 34F/34R

22

457   (Supplementary Table 4). We transformed *B. cinerea* using PEG mediated transformation.

458   0.125% lysing enzyme from Trichoderma harzianum (Sigma–Aldrich, Germany) was used for

459   protoplast generation. Following transformation, protoplasts were plated on SH medium

460   (sucrose, Tris-Cl, $(NH_4)_2HPO_4$ and 35µg/ ml hygromycin B). Colonies that grew after 2 days

461   were transferred to PDA-hygromycin, and conidia were re-spread on selection plates to obtain a

462   monoconidial culture. Transformants were visualized under a confocal microscope and screened

463   with primers GA 44F/44R and GA 31F/31R (Supplementary Table 4). Confirmed transformants

464   were stored at 80°C and used for further experiments. Confocal microscopy images were

465   acquired using an Olympus 398 IX 81 confocal microscope (Fluoview 500) equipped with a 60×

466   1.0 NA PlanApo water immersion objective. eGFP images were acquired using a 488 nm

467   excitation laser (1% power), with emission collected in the range 488-509 nm. Corrected total

468   fluorescence was quantified using ImageJ.

469   *B. cinerea* **endocytosis**

470   *Bc* hyphae were grown in PDB with or without 6-BAP (100nM, 100 µM), Benomyl (sigma, cat

471   no. 17804-35-2), or LatrunculinB (sigma, cat no. 76343-94-7) for 16 h at 22 °C, after which the

472   cells were collected and stained with 5 µM FM4-64 on a glass coverslip. We acquired confocal

473   microscopy images using a Zeiss LSM780 confocal microscope equipped with a 63×/1.15 Corr

474   Objective. FM-4-64 images were acquired with a 514 nm excitation laser (4% power), with the

475   emission collected in the range of 592–768 nm. Images of 8 bits and 1024 × 1024 pixels were

476   acquired using a pixel dwell time of 1.27, pixel averaging of 4, and pinhole of 1 airy unit (1.3

477   µM). Image analysis (18-24 images per treatment collected in three independent experiments)

478   was conducted with Fiji-ImageJ using the raw images and the 3D object counter tool and

479   measurement analysis tool (Schindelin *et al.*, 2012). Endosome density and size were calculated

480   automatically by the software tool considering 1.3 µM depth, based on single optical sections.

481   **Budding (*Saccharomyces cerevisiae*) and fission (*Schizosaccharomyces pombe*) yeast growth**

23

482   Wild-type haploid yeast strains were grown over night at 30°C. *S. cerevisiae* cells were grown in

483   synthetic defined (SD) medium and *S. pombe* cells were grown in Edinburgh minimal medium

484   (EMM), without (mock) or with the addition of indicated concentrations of CK (6-BAP). *S.*

485   *cerevisiae* and *S. pombe* were diluted to an OD_{600} of 0.01. 200 µL of cells were plated in 96 well

486   plates and incubated at 30°C for 25h (*S. cerevisiae*) or 45h (*S. pombe*), with continuous shaking.

487   OD_{600} was measured using a TecanTM SPARK 10M plate reader. Experiment was repeated three

488   times with similar results. WT strains of *S. cerevisiae* and *S. pombe* were kind gifts from Martin

489   Kupiec and Ronit Weisman.

490   **Budding (*S. cerevisiae*) and fission (*S. pombe*) yeast endocytosis**

491   *Saccharomyces cerevisiae* was grown overnight in YPD media, then the culture was diluted

492   ($OD_{600} = 0.2$) and incubated for 6 hours in YPD (mock) or YPD supplemented with 300 µM 6-

493   BAP. *Saccharomyces pombe* was grown overnight in YE. The cultures were then diluted (OD_{600}

494   = 0.2) and incubated for 6 hours in YE media (mock) or media supplemented with 100 µM 6-

495   BAP. Cell cultures were collected by centrifugation at 5,000 rpm for 4 minutes, and re-suspended

496   in fresh growth medium. FM4-64 staining was performed as described (Vásquez-Soto *et al.*,

497   2015). Cells were incubated with 24 µM FM4-64 (Invitrogen) for 30 min at 4°C. Subsequently,

498   the FM4-64 containing medium was replaced with fresh medium, and cultures was incubated for

499   15 minutes at 28°C. To observe FM4-64 distribution, 5 µl of the suspensions were placed on a

500   slide and live confocal imaging was performed. Confocal microscopy images were acquired

501   using a Zeiss LSM780 confocal microscope equipped with Objective LD C-Apochromat

502   63×/1.15 Corr. Acquisition settings were designed using an excitation laser wavelength of 514

503   nm (4% power). The emission was then collected in the range of 592–768 nm. Images of 8 bits

504   and 1024×1024 were acquired using a pixel dwell time of 1.27, pixel averaging of 4 and pinhole

505   of 1 airy unit. Bright field was acquired using the T-PMT (transmitted light detector). Image

506   analysis was performed using Fiji-ImageJ with the raw images (Schindelin *et al.*, 2012),

507 endosome count and size measurements were performed with the 3D Object counter tool and

508 pixel intensity was measured using the measurement analysis tool.

509 **Construction of budding yeast mutant strains**

510 The *YPT31, SSA1, VPS1 and SPO14* genes were disrupted in wild-type yeast strain (BY4741)

511 via homologous recombination using PCR fragments amplified from the plasmid pFA6a-

512 KanMX6 as a template with suitable primers. Gene replacement was validated by PCR with

513 suitable primers. Primer sequences are provided in Supplemental Table 3.

514 **Data analysis**

515 All data is presented as the average ±SEM. We analyzed the statistical significance of differences

516 between two groups using a two-tailed t-test, with additional post hoc correction where

517 appropriate, such as FDR calculation with Holm-Sidak correction, and Welch's correction for t-

518 tests between samples with unequal variance. We analyzed the statistical significance of

519 differences among three or more groups using analysis of variance (ANOVA). Regular ANOVA

520 was used for groups with equal variances, and Welch's ANOVA for groups with unequal

521 variances. Significance in differences between the means of different samples in a group of 3 or

522 more samples was assessed using a post-hoc test. The Tukey post-hoc test was used for samples

523 with equal variances, when the mean of each sample was compared to the mean of every other

524 sample. The Bonferroni post-hoc test was used for samples with equal variances, when the mean

525 of each sample was compared to the mean of a control sample. The Dunnett post-hoc test was

526 used for samples with unequal variances. Statistical analyses were conducted using Prism8^{TM}.

527

528 **Acknowledgements**

535   **Author contributions**

536   Conceptualization: MB, RG. Design: RG, LP, GA, DL, TY, MB. Methodology &
537   experimentation: RG, LP, GA, DL, NK. Analysis: RG, LP, GA, DL, NS, UG, MB. Manuscript:
538   RG, LP, GA, DL, UG, MB.

539   **The authors declare no competing interest.**

540   **Data availability statement**

541   The authors declare that the data supporting the findings of this study are available within the

542   paper and its supplementary information files. Raw data is available from the corresponding

543   author upon reasonable request.

References

544 **Aguayo C, Riquelme J, Valenzuela PDT, Hahn M, Silva Moreno E**. **2011**. Bchex

545 virulence gene of Botrytis cinerea: characterization and functional analysis. *Journal of*

546 *General Plant Pathology* **77**: 230–238.

547 **Argueso CT, Ferreira FJ, Epple P, To JPC, Hutchison CE, Schaller GE, Dangl JL,**

548 **Kieber JJ**. **2012**. Two-component elements mediate interactions between cytokinin and

549 salicylic acid in plant immunity. *PLoS Genetics* **8**.

550 **Arnold GRW**. **2008**. Farr, D. F.; Bills, G. F.; Chamuris, G. P.; Rossman, A. Y., Fungi on

551 Plants and Plant Products in the United States. VIII, 1252 S. The American

552 Phytopathological Society (APS) Press, St. Paul (Minnesota), 1989. ISBN 0-89054-099-3.

553 *Feddes Repertorium* **101**: 340–340.

554 **Babosha A V. 2009**. Regulation of resistance and susceptibility in wheat-powdery mildew

555 pathosystem with exogenous cytokinins. *Journal of Plant Physiology* **166**: 1892–1903.

556 **Ballaré CL**. **2011**. Jasmonate-induced defenses: a tale of intelligence, collaborators and

557 rascals. *Trends in Plant Science* **16**: 249–257.

558 **Bartnicki-Garcia S**. **2002**. Hyphal Tip Growth Outstanding Questions. *Published in*

559 *"Molecular Biology of Fungal Development" (H. D. Osiewacz, ed.).*: 29–58.

560 **Berepiki A, Lichius A, Read ND**. **2011**. Actin organization and dynamics in filamentous

561 fungi. *Nature Reviews Microbiology* **9**: 876–887.

562 **Bolger AM, Lohse M, Usadel B**. **2014**. Trimmomatic: A flexible trimmer for Illumina

563 sequence data. *Bioinformatics* **30**: 2114–2120.

564 **Boucrot E, Saffarian S, Massol R, Kirchhausen T, Ehrlich M**. **2006**. Role of lipids and

565 actin in the formation of clathrin-coated pits. *Experimental cell research* **312**: 4036–48.

566 **Bradford MM**. **1976**. A rapid and sensitive method for the quantitation of microgram

567 quantities of protein utilizing the principle of protein-dye binding. *Analytical Biochemistry*

568 **72**: 248–254.

569 **Brito N, Espino JJ, González C**. **2006**. The endo-beta-1,4-xylanase xyn11A is required for

570 virulence in Botrytis cinerea. *Molecular plant-microbe interactions : MPMI* **19**: 25–32.

571 **Buchfink B, Xie C, Huson DH**. **2014**. Fast and sensitive protein alignment using

572   DIAMOND. *Nature Methods* **12**: 59–60.

573   **De Cal A, Garcia-Lepe R, Melgarejo P**. **2000**. Induced Resistance by Penicillium

574   oxalicum Against Fusarium oxysporum f. sp. lycopersici: Histological Studies of Infected

575   and Induced Tomato Stems. *Am Phytopath Society*.

576   **Choi J, Choi D, Lee S, Ryu C-M, Hwang I**. **2011**. Cytokinins and plant immunity: old

577   foes or new friends? *Trends in Plant Science* **16**: 388–394.

578   **Choi J, Huh SU, Kojima M, Sakakibara H, Paek K-HH, Hwang I**. **2010**. The cytokinin-

579   activated transcription factor ARR2 promotes plant immunity via TGA3/NPR1-dependent

580   salicylic acid signaling in arabidopsis. *Developmental Cell* **19**: 284–295.

581   **Conesa A, Götz S, García-Gómez JM, Terol J, Talón M, Robles M**. **2005**. Blast2GO: A

582   universal tool for annotation, visualization and analysis in functional genomics research.

583   *Bioinformatics* **21**: 3674–3676.

584   **Dean R, van Kan J, Pretorius Z, Hammond-Kosack K, Di pietro A, Spanu P, Redd J,**

585   **Dickman M, Kahmann R, Ellis J, *et al.*** **2012**. The Top 10 fungal pathogens in molecular

586   plant pathology. *Molecular Plant Pathology* **13**: 414–430.

587   **Dobin A, Davis CA, Schlesinger F, Drenkow J, Zaleski C, Jha S, Batut P, Chaisson M,**

588   **Gingeras TR**. **2013**. STAR: Ultrafast universal RNA-seq aligner. *Bioinformatics* **29**: 15–

589   21.

590   **Dub AM, Kokkelink L, Tudzynski B, Tudzynski P, Sharon A**. **2013**. Involvement of

591   Botrytis cinerea small GTPases BcRAS1 and BcRAC in differentiation, virulence, and the

592   cell cycle. *Eukaryotic Cell* **12**: 1609–1618.

593   **Ekena K, Vater CA, Raymond CK, Stevens TH**. **1993**. The VPS1 protein is a dynamin-

594   like GTPase required for sorting proteins to the yeast vacuole. *Ciba Foundation symposium*

595   **176**.

596   **Fillinger S, Elad Y**. **2016**. *Botrytis -- the fungus, the pathogen and its management in*

597   *agricultural systems*.

598   **Fischer-Parton S, Parton RM, Hickey PC, Dijksterhuis J, Atkinson HA, Read ND**.

599   **2000**. Confocal microscopy of FM4-64 as a tool for analysing endocytosis and vesicle

600   trafficking in living fungal hyphae. *Journal of Microscopy* **198**: 246–259.

601 **Frías M, González M, González C, Brito N**. **2019**. A 25-Residue Peptide From Botrytis

602 cinerea Xylanase BcXyn11A Elicits Plant Defenses. *Frontiers in Plant Science* **10**: 474.

603 **Gentleman RC, Carey VJ, Bates DM, Bolstad B, Dettling M, Dudoit S, Ellis B, Gautier**

604 **L, Ge Y, Gentry J,** *et al.* **2004**. Bioconductor: open software development for

605 computational biology and bioinformatics. *Genome biology* **5**.

606 **Ghanem ME, Albacete A, Martínez-Andújar C, Acosta M, Romero-Aranda R, Dodd**

607 **IC, Lutts S, Pérez-Alfocea F**. **2008**. Hormonal changes during salinity-induced leaf

608 senescence in tomato (Solanum lycopersicum L.). *Journal of Experimental Botany* **59**:

609 3039–3050.

610 **Gomes CJ, Harman MW, Centuori SM, Wolgemuth CW, Martinez JD**. **2018**.

611 Measuring DNA content in live cells by fluorescence microscopy. *Cell Division* **13**: 6.

612 **Gourgues M, Brunet-Simon A, Lebrun M-H, Levis C**. **2004**. The tetraspanin BcPls1 is

613 required for appressorium-mediated penetration of Botrytis cinerea into host plant leaves.

614 *Molecular microbiology* **51**: 619–29.

615 **Greene EM**. **1980**. Cytokinin production by microorganisms. *The Botanical Review* **46**:

616 25–74.

617 **Grosskinsky DK, Naseem M, Abdelmohsen UR, Plickert N, Engelke T, Griebel T,**

618 **Zeier J, Novak O, Strnad M, Pfeifhofer H,** *et al.* **2011**. Cytokinins Mediate Resistance

619 against Pseudomonas syringae in Tobacco through Increased Antimicrobial Phytoalexin

620 Synthesis Independent of Salicylic Acid Signaling. *Plant Physiology* **157**: 815–830.

621 **Gupta R, Leibman-Markus M, Pizarro L, Bar M**. **2020a**. Cytokinin induces bacterial

622 pathogen resistance in tomato. *Plant Pathology* **In press**.

623 **Gupta R, Pizarro L, Leibman-Markus M, Marash I, Bar M**. **2020b**. Cytokinin response

624 induces immunity and fungal pathogen resistance, and modulates trafficking of the PRR

625 LeEIX2 in tomato. *Molecular plant pathology*: 10.1111/mpp.12978.

626 **Hérivaux A, Dugé de Bernonville T, Roux C, Clastre M, Courdavault V, Gastebois A,**

627 **Bouchara J-P, James TY, Latgé J-P, Martin F,** *et al.* **2017**. The Identification of

628 Phytohormone Receptor Homologs in Early Diverging Fungi Suggests a Role for Plant

629 Sensing in Land Colonization by Fungi. *mBio* **8**.

630 **Jameson PE**. **2000**. Cytokinins and auxins in plant-pathogen interactions – An overview.

631   *Plant Growth Regulation* **32**: 369–380.

632   **Jedd G, Mulholland J, Segev N**. **1997**. Two new Ypt GTPases are required for exit from

633   the yeast trans-Golgi compartment. *The Journal of cell biology* **137**: 563–80.

634   **Ji D, Chen T, Ma D, Liu J, Xu Y, Tian S**. **2018**. Inhibitory effects of methyl thujate on

635   mycelial growth of Botrytis cinerea and possible mechanisms. *Postharvest Biology and*

636   *Technology* **142**: 46–54.

637   **Jia Y, Li W**. **2018**. Phospholipase D antagonist 1-butanol inhibited the mobilization of

638   triacylglycerol during seed germination in Arabidopsis. *Plant diversity* **40**: 292–298.

639   **Keshishian EA, Rashotte AM**. **2015**. Plant cytokinin signalling. *Essays in biochemistry*

640   **58**: 13–27.

641   **Ketelaar T, Meijer HJG, Spiekerman M, Weide R, Govers F**. **2012**. Effects of

642   latrunculin B on the actin cytoskeleton and hyphal growth in Phytophthora infestans.

643   *Fungal Genetics and Biology* **49**: 1014–1022.

644   **Krantz KC, Puchalla J, Thapa R, Kobayashi C, Bisher M, Viehweg J, Carr CM, Rye**

645   **HS**. **2013**. Clathrin coat disassembly by the yeast Hsc70/Ssa1p and auxilin/Swa2p proteins

646   observed by single-particle burst analysis spectroscopy. *The Journal of biological chemistry*

647   **288**: 26721–30.

648   **Laor D, Sade D, Shaham-Niv S, Zaguri D, Gartner M, Basavalingappa V, Raveh A,**

649   **Pichinuk E, Engel H, Iwasaki K,** *et al.* **2019**. Fibril formation and therapeutic targeting of

650   amyloid-like structures in a yeast model of adenine accumulation. *Nature Communications*

651   **10**: 1–11.

652   **Lewis J, Papavizas G**. **1987**. Permeability changes in hyphae of Rhizoctonia solani

653   induced by germling preparations of Trichoderma and Gliocladium. *Physiology and*

654   *Biochemistry* **77**: 699–703.

655   **Li X, Gao M, Han X, Tao S, Zheng D, Cheng Y, Yu R, Han G, Schmidt M, Han L**.

656   **2012**. Disruption of the phospholipase D gene attenuates the virulence of Aspergillus

657   fumigatus. *Infection and immunity* **80**: 429–40.

658   **Liarzi O, Benichis M, Gamliel A, Ezra D**. **2020**. *trans* -2-Octenal, a single compound of a

659   fungal origin, controls *Sclerotium rolfsii* , both *in vitro* and in soil. *Pest Management*

660   *Science* **76**: 2068–2071.

661   **Liu Z, Bushnell WR**. **1986**. Effects of cytokinins on fungus development and host

662   response in powdery mildew of barley. *Physiological and Molecular Plant Pathology* **29**:

663   41–52.

664   **Llanos A, François JM, Parrou JL**. **2015**. Tracking the best reference genes for RT-qPCR

665   data normalization in filamentous fungi. *BMC Genomics* **16**: 71.

666   **Love MI, Huber W, Anders S**. **2014**. Moderated estimation of fold change and dispersion

667   for RNA-seq data with DESeq2. *Genome Biology* **15**.

668   **Marhavý P, Bielach A, Abas L, Abuzeineh A, Duclercq J, Tanaka H, Pařezová M,**

669   **Petrášek J, Friml J, Kleine-Vehn J,** *et al.* **2011**. Cytokinin Modulates Endocytic

670   Trafficking of PIN1 Auxin Efflux Carrier to Control Plant Organogenesis. *Developmental*

671   *Cell* **21**: 796–804.

672   **Mes J, Weststeijn E, Herlaar F**. **1999**. Biological and Molecular Characterization of

673   Fusarium oxysporum f. sp. lycopersici Divides Race 1 Isolates into Separate Virulence

674   Groups. *Am Phytopath Society*.

675   **Mishina GN, Talieva MN, Babosha AV, Serezhkina GV, Andreev LN**. **2002**. Influence

676   of phytohormones on development of conidial inoculum of causative agents of the phlox

677   and barley powdery mildew | Vliianie fitogormonov na razvitie konidial'nogo inokuliuma

678   vozbuditelei muchnistoi rosy floksa i iachmenia. *Izvestiia Akademii nauk. Seriia*

679   *biologicheskaia / Rossiiskaia akademiia nauk* **29**: 46–52.

680   **Mok DW, Mok MC**. **2001**. Cytokinin metabolism and action. *Ann. Rev. Plant Physiol.*

681   *Plant Mol. Biol.* **52**: 89–118.

682   **Momany M, Hamer JE**. **1997**. Relationship of actin, microtubules, and crosswall synthesis

683   during septation in Aspergillus nidulans. *Cell Motility and the Cytoskeleton* **38**: 373–384.

684   **Motes CM, Pechter P, Yoo CM, Wang Y-S, Chapman KD, Blancaflor EB**. **2005**.

685   Differential effects of two phospholipase D inhibitors, 1-butanol and N-acylethanolamine,

686   on in vivo cytoskeletal organization and Arabidopsis seedling growth. *Protoplasma* **226**:

687   109–123.

688   **Naseem M, Philippi N, Hussain A, Wangorsch G, Ahmed N, Dandekar T, Dandekara**

689   **T, Dandekar T**. **2012**. Integrated systems view on Networking by hormones in Arabidopsis

690   immunity reveals multiple crosstalk for cytokinin. *The Plant Cell* **24**: 1793–1814.

691 **Nieto K, Frankenberger W**. **1991**. Microbial production of cytokinins. Soil biochemistry.

692 Volume 6., 191-248. Bollag, J.-M. and G. Stotzky (eds.): Soil Biochemistry, Vol. 6 (Books

693 in Soils, Plants, and the Environment Series). *Zeitschrift für Pflanzenernährung und*

694 *Bodenkunde* **154**: 74–74.

695 **Peterson JR, Mitchison TJ**. **2002**. Small molecules, big impact: A history of chemical

696 inhibitors and the cytoskeleton. *Chemistry and Biology* **9**: 1275–1285.

697 **Pfaffl MW**. **2001**. A new mathematical model for relative quantification in real-time RT-

698 PCR. *Nucleic Acids Res* **29**: e45.

699 **Riquelme M, Aguirre J, Bartnicki-García S, Braus GH, Feldbrügge M, Fleig U,**

700 **Hansberg W, Herrera-Estrella A, Kämper J, Kück U,** *et al.* **2018**. Fungal

701 Morphogenesis, from the Polarized Growth of Hyphae to Complex Reproduction and

702 Infection Structures. *Microbiology and molecular biology reviews : MMBR* **82**.

703 **Rudge SA, Zhou C, Engebrecht JA**. **2002**. Differential regulation of Saccharomyces

704 cerevisiae phospholipase D in sporulation and Sec14-independent secretion. *Genetics* **160**:

705 1353–1361.

706 **Sakakibara H**. **2006**. Cytokinins: Activity, Biosynthesis, and Translocation. *Annu Rev*

707 *Plant Biol*.

708 **Schindelin J, Arganda-Carreras I, Frise E, Kaynig V, Longair M, Pietzsch T,**

709 **Preibisch S, Rueden C, Saalfeld S, Schmid B,** *et al.* **2012**. Fiji: an open-source platform

710 for biological-image analysis. *Nature Methods* **9**: 676–682.

711 **Schumacher J**. **2012**. Tools for Botrytis cinerea: New expression vectors make the gray

712 mold fungus more accessible to cell biology approaches. *Fungal Genetics and Biology* **49**:

713 483–497.

714 **Schumacher J, Viaud M, Simon A, Tudzynski B**. **2008**. The Gα subunit BCG1, the

715 phospholipase C (BcPLC1) and the calcineurin phosphatase co-ordinately regulate gene

716 expression in the grey mould fungus Botrytis cinerea. *Molecular Microbiology* **67**: 1027–

717 1050.

718 **Sharfman M, Bar M, Ehrlich M, Schuster S, Melech-Bonfil S, Ezer R, Sessa G, Avni**

719 **A**. **2011**. Endosomal signaling of the tomato leucine-rich repeat receptor-like protein

720 LeEix2. *The Plant Journal* **68**: 413–423.

721 **Sharma N, Rahman MH, Liang Y, Kav NN V. 2010**. Cytokinin inhibits the growth of
722 *Leptosphaeria maculans* and *Alternaria brassicae*. *Canadian Journal of Plant Pathology*
723 **32**: 306–314.

724 **Silva-Moreno E, Brito-Echeverría J, López M, Ríos J, Balic I, Campos-Vargas R,**
725 **Polanco R**. **2016**. Effect of cuticular waxes compounds from table grapes on growth,
726 germination and gene expression in Botrytis cinerea. *World Journal of Microbiology and*
727 *Biotechnology* **32**: 74.

728 **Sørensen JL, Benfield AH, Wollenberg RD, Westphal K, Wimmer R, Nielsen MR,**
729 **Nielsen KF, Carere J, Covarelli L, Beccari G,** *et al.* **2018**. The cereal pathogen Fusarium
730 pseudograminearum produces a new class of active cytokinins during infection. *Molecular*
731 *Plant Pathology* **19**: 1140–1154.

732 **Staats M, van Kan JAL**. **2012**. Genome update of Botrytis cinerea strains B05.10 and T4.
733 *Eukaryotic Cell* **11**: 1413–1414.

734 **Stravato VM, Buonaurio R, Cappelli C**. **1999**. First Report of *Fusarium oxysporum* f. sp.
735 *lycopersici* Race 2 on Tomato in Italy. *Plant Disease* **83**: 967–967.

736 **Suzuki T, Miwa K, Ishikawa K, Yamada H, Aiba H, Mizuno T**. **2001**. The Arabidopsis
737 sensor kinase, AHK4, can respond to cytokinin. *Plant Cell Physiol.* **42**: 107–113.

738 **Swartzberg D, Kirshner B, Rav-David D, Elad Y, Granot D**. **2008**. Botrytis cinerea
739 induces senescence and is inhibited by autoregulated expression of the IPT gene. *European*
740 *Journal of Plant Pathology* **120**: 289–297.

741 **Torres-Ossandón MJ, Vega-Gálvez A, Salas CE, Rubio J, Silva-Moreno E, Castillo L**.
742 **2019**. Antifungal activity of proteolytic fraction (P1G10) from (Vasconcellea
743 cundinamarcensis) latex inhibit cell growth and cell wall integrity in Botrytis cinerea.
744 *International Journal of Food Microbiology* **289**: 7–16.

745 **Trapnell C, Roberts A, Goff L, Pertea G, Kim D, Kelley DR, Pimentel H, Salzberg SL,**
746 **Rinn JL, Pachter L**. **2012**. Differential gene and transcript expression analysis of RNA-seq
747 experiments with TopHat and Cufflinks. *Nature Protocols* **7**: 562–578.

748 **Tsahouridou PC, Thanassoulopoulos CC**. **2002**. Proliferation of Trichoderma koningii in
749 the tomato rhizosphere and the suppression of damping-off by Sclerotium rolfsii. *Soil*
750 *Biology and Biochemistry* **34**: 767–776.

751 **Valette-Collet O, Cimerman A, Reignault P, Levis C, Boccara M**. **2003**. Disruption of
752 Botrytis cinerea pectin methylesterase gene Bcpme1 reduces virulence on several host
753 plants. *Molecular plant-microbe interactions : MPMI* **16**: 360–7.

754 **Vásquez-Soto B, Manríquez N, Cruz-Amaya M, Zouhar J, Raikhel N V, Norambuena**
755 **L**. **2015**. Sortin2 enhances endocytic trafficking towards the vacuole in Saccharomyces
756 cerevisiae. *Biological Research* **48**: 39.

757 **Vater CA, Raymond CK, Ekena K, Howald-Stevenson I, Stevens TH**. **1992**. The VPS1
758 protein, a homolog of dynamin required for vacuolar protein sorting in Saccharomyces
759 cerevisiae, is a GTPase with two functionally separable domains. *Journal of Cell Biology*
760 **119**: 773–786.

761 **Vrabka J, Niehaus E-M, Münsterkötter M, Proctor RH, Brown DW, Novák O, Pěnčik**
762 **A, Tarkowská D, Hromadová K, Hradilová M, *et al.* 2018**. Production and Role of
763 Hormones During Interaction of Fusarium Species With Maize (Zea mays L.) Seedlings.
764 *Frontiers in plant science* **9**: 1936.

765 **Walker SK, Garrill A**. *Actin microfilaments in fungi*.

766 **Walters DR, McRoberts N**. **2006**. Plants and biotrophs: a pivotal role for cytokinins?
767 *Trends in plant science* **11**: 581–6.

768 **Wang Y, Liu X, Chen T, Xu Y, Tian S**. **2020**. Antifungal effects of hinokitiol on
769 development of Botrytis cinerea in vitro and in vivo. *Postharvest Biology and Technology*
770 **159**: 111038.

771 **Wellman F**. **1939**. A technique for sutdying host resistance and pathogenicity in tomato
772 Fusarium wilt. *Phytopathology*.

773 **Werner T, Schmülling T**. **2009**. Cytokinin action in plant development. *Current opinion in*
774 *plant biology* **12**: 527–38.

775 **Williamson B, Tudzynski B, Tudzynski P, Van Kan JAL**. **2007**. Botrytis cinerea: The
776 cause of grey mould disease. *Molecular Plant Pathology* **8**: 561–580.

777 **Xie C, Mao X, Huang J, Ding Y, Wu J, Dong S, Kong L, Gao G, Li CY, Wei L**. **2011**.
778 KOBAS 2.0: A web server for annotation and identification of enriched pathways and
779 diseases. *Nucleic Acids Research* **39**.

780   **Zheng L, Campbell M, Murphy J, Lam S, Xu JR**. **2000**. The BMP1 gene is essential for

781   pathogenicity in the gray mold fungus Botrytis cinerea. *Molecular plant-microbe*

782   *interactions : MPMI* **13**: 724–32.

783   **Žižková E, Dobrev PI, Muhovski Y, Hošek P, Hoyerová K, Haisel D, Procházková D,**

784   **Lutts S, Motyka V, Hichri I**. **2015**. Tomato (Solanum lycopersicum L.) SlIPT3 and

785   SlIPT4 isopentenyltransferases mediate salt stress response in tomato. *BMC Plant Biology*

786   **15**: 1–20.

Figure legends

787

Fig. 1. Direct effect of cytokinin on fungal growth and disease.

789   **(a)-(c)** *S. lycopersicum* cv M82 leaves were treated with 100 µM CK (6-BAP; 6-

790   Benzylaminopurine) and inoculated with indicated pathogens 24 hours later. Plant disease was

791   quantified as indicated in the material and methods section, disease in the mock treatment was set

792   to 1. Graphs represent results from 4-6 biological repeats ±SE, N>40. Asterisks represent significant

793   difference among means in a two-tailed t-test, ****$p<0.0001$, ns-non-significant. All individual

794   values plotted, purple bar represents mean ±SE.

795   **(d)-(i)** *B. cinerea, S. rolfsii and F. oxysporum* were cultured on potato dextrose agar (PDA) plates

796   in the presence of 100 µM 6-BAP. **(j)** Quantification of results from 4-6 biological repeats ±SE,

797   including adenine (100 µM) as a control, N>20. Asterisks (differences between Mock and CK) and

798   letters (differences between the level of CK growth inhibition in the different fungi) indicate

799   significance in one-way ANOVA with a Bonferroni post hoc test, *$p<0.05$, **$p<0.01$,

800   ****$p<0.0001$, ns=non-significant. **(k)** *B. cinerea* was cultured on potato dextrose agar (PDA) plates

801   in the presence of 100 µM of the indicated CK compound (TDZ=Thidiazuron). Quantification of

802   results from 3 biological repeats ±SE, N=12. Asterisks indicate significance in one-way ANOVA

803   with a Tukey post hoc test, ***$p<0.001$, ****$p<0.0001$. **(i-k)** Dose response of *B. cinerea, S. rolfsii*

804   *and F. oxysporum* to CK- different concentrations of 6-BAP as indicated. Graphs represent 3

805   biological repeats ±SE, N>6. Letters indicate significance in a one-way ANOVA, ****$p<0.0001$ in

806   all cases, with a Tukey post-hoc test. **j-k**: Box-plot displays minimum to maximum values, with

807   inner quartile ranges indicated by box and outer-quartile ranges by whiskers. Line indicates median,

808   dot indicates mean.

809

810 **Fig. 2. Cytokinin inhibits *Bc* sporulation and spore germination.**

811 **(a)-(b)** *B. cinerea* was cultured on PDA plates or PDB liquid broth in the presence of 100 nM or 100

812 µM 6-Benzylaminopurine (6-BAP). Spore formation is indicated by dark color **(a)** and quantified in

813 **(b)**. Spore germination and germ tube elongation are demonstrated in **(c)** with calcofluor staining

814 (scale bar = 20 µM), and quantified in **(d)-(e)**. **(b,d,e)** Quantification of results from 4 biological

815 repeats ±SE, N>25. Asterisks or letters indicate significance in one-way ANOVA with a Tukey post

816 hoc test, ***$p<0.005$, ****$p<0.001$. Individual values graphed, blue bar represents mean ±SE.

817

818 **Fig. 3. Cytokinin inhibits *B. cinerea* virulence.**

819 **(a)** Infectivity of spores sporulated from mycelia grown with or without cytokinin (CK; 6-

820 Benzylaminopurine). Spores were harvested in a glucose/potassium media as described in the

821 materials sections, and diluted to an equal concentration (the CK grown spores were concentrated

822 as CK grown fungi produce reduced numbers). **(b)** Infectivity of spores grown in rich media and

823 harvested from the same plate; half the spores were mixed with CK prior to infection. **(c)** *B. cinerea*

824 was grown in PDB with the addition of 100 µM CK (6-BAP) or without (Mock). qRT-PCR was

825 carried out on the virulence genes *BMP1, PME, PLS1, PLC1, PG1, hex, XynI, Xyn10A* and *Xyn11C*.

826 Mock was set to 1. Gene expression values were normalized to a geometric mean of the expression

827 of 3 housekeeping genes: Ubiquitin-conjugating enzyme E2, Iron-transport multicopper oxidase,

828 and Adenosine deaminase. Graph represents 3 biological repeats, N=9. **a-b:** individual values

829 graphed, pink bar represents mean ±SE. Results were analyzed for statistical significance using a

830 two-tailed t-test, ****$p<0.0001$; ns-non-significant. **c:** floating bars, line indicates mean. Results

831 were analyzed for statistical significance using Welch's Anova with a Dunnett post hoc test, *$p<0.05$,

832 **$p<0.01$, ****$p<0.0001$.

833

834 **Fig. 4. Cytokinin is not toxic to *B. cinerea*.**

835 *B. cinerea* (*Bc*) was cultured in PDB liquid broth, with or without 100 µM CK (6-

836 Benzylaminopurine). After 24 hours, protein leakage **(a)**, nucleic acid leakage **(b)**, and media

837 conductivity **(c)** were measured. Graphs represent 3 biological repeats ±SE, N>6. Letters indicate

838 significance in one-way ANOVA with a Tukey (a) or Bonferroni (b,c) post hoc test; a p=ns; b,c

839 $p<0.0001$. Box-plot with 2.5% whiskers; line indicates median, dot indicates mean. No significant

840 difference between control media containing CK (without *Bc*) or *Bc* with CK was observed in any

841 of the parameters.

842

843 **Fig. 5. Transcriptomics reveal fungal pathways affected by CK**

844 Analysis of Illumina Hiseq NGS of *Bc* samples Mock treated or CK treated (25 uM), 3 biological

845 repeats each. Gene expression values were computed as FPKM. Differential expression analysis was

846 completed using the DESeq2 R package. Genes with an adjusted p-value of no more than 0.05 and

847 log2FC greater than 1 or lesser than -1 were considered differentially expressed. **(a)** Principle

36

848   component analysis (PCA) of 3 biological repeats from each treatment. PCA was calculated using
849   the R function prcomp. **(b)** Heatmap depicting the clustering of the different samples in terms of
850   differentially expressed genes. Blue= negatively regulated by CK, red= positively regulated by CK.
851   Color saturation indicates strength of differential expression. Heatmap visualization was performed
852   using R Bioconductor. See also Supplemental data 1. **(c-d)** Analysis of statistically enriched
853   pathways downregulated (c, blue) and upregulated (d, red) by CK. KOBAS 3.0 tool was used to
854   detect the statistical enrichment of differential expression genes in Kyoto Encyclopedia of Genes
855   and Genomes (KEGG) pathways and Gene Ontology (GO). Pathways were tested for significant
856   enrichment using Fisher's exact test, with Benjamini and Hochberg FDR correction. Corrected p-
857   value was deemed significant at $p<0.05$. See also Supplemental data 2 and 3. In (c-d), the darker the
858   color the higher the number of DEGs in a pathway, and the bigger the letters, the higher percentage
859   of the pathway that is differential.

861   **Fig. 6. Cytokinin reduces *B. cinerea* cell elongation and DNA replication**
862   *B. cinerea* was cultured in PDB liquid broth, with or without 100 µM CK (6-Benzylaminopurine).
863   After 8 **(f)** or 16 hours **(a-e,g)**, growing hyphae were stained with calcofluor **(a,b,d,e,f)** or hoechst
864   **(c,g)**, and imaged on an Olympus IX 81 confocal laser scanning microscope using a 405nm diode
865   laser (1% power), under identical imaging conditions. **a-c:** bar=50 µM; **b:** bar=20 µM. Cell area **(d)**,
866   distance between septa **(e)**, No. of septa in individual germinated hyphae **(f)** and DNA staining **(g)**
867   were measured using Fiji-ImageJ. Graphs represent 3-6 biological repeats, N>120 (d,e), N>30 (f),
868   N=170 (g). Statistically significant differences between Mock and CK samples were assessed using
869   a two-tailed t-test, ****$p<0.0001$. Individual values graphed, blue bar represents mean ±SE.

871   **Fig. 7. Cytokinin inhibits the fungal cytoskeleton**

872   **(a)** Cytoskeleton related *B. cinerea* genes found to be differentially regulated in the RNAseq. See
873   Supplemental data 4 for full list. **(b)** qRT-PCR validation of expression levels of 5 cytoskeleton
874   related genes upon CK treatment. *B. cinerea* was grown in PDB with the addition of 100 µM CK
875   (6-BAP) or without (Mock). Mock was set to 1. Gene expression values were normalized to a
876   geometric mean of the expression of 3 housekeeping genes: Ubiquitin-conjugating enzyme E2, Iron-
877   transport multicopper oxidase, and Adenosine deaminase. Floating bars represent minimum to
878   maximum values of 3 biological repeats, line represents mean. Asterisks indicate significance in a
879   two-tailed t-test with Welch's correction, *$p<0.05$; ***$p<0.001$. **(c-d)** *B. cinerea* was transformed
880   with lifeactin-GFP. Germinated spores were treated with Mock or CK and grown for 6 h prior to
881   confocal visualization. **(c)** Representative images, bar=10 uM. **(d)** Analysis of corrected total
882   fluorescence (CTF) of the ratio between life-actin at the tip of the cell and the total cell in Mock and
883   CK treated cells. Three independent experiments were conducted with a total of 30 images analyzed,
884   N>80 growing hyphae tips. Asterisks indicate significance in a two-tailed t-test with Welch's
885   correction, ****$p<0.0001$.

37

Fig. 8. Cytokinin inhibits FM-4-64 endocytosis in growing *B. cinerea* hyphae.

B. cinerea (*Bc*) was cultured in PDB liquid broth in the presence of 100 nM or 100 µM CK (6-Benzylaminiopurine) for 16 hours. **(a)** FM-4-64 endocytic vesicles in *Bc* hyphae. **(b)** quantification of the amount of endocytic vesicles; **(c)** quantification of the average size of vesicles. Measurements were done using the counting tool of Fiji. Quantification of results from 7 biological repeats. **b:** N>45, box-plot with all values displayed, box indicates inner-quartile ranges with line indicating median, whiskers indicate outer-quartile ranges. **c:** N>450, all values displayed, line indicates median ±SE. Asterisks indicate significance in one-way ANOVA with a Tukey post hoc test, *p<0.05; **p<0.01; ****p<0.0001; ns- non-significant.

Fig. 9. Cytokinin inhibits growth and endocytosis in budding yeast.

(a) Wild-type *Saccharomyces cerevisiae* were grown over night at 30°C in minimal synthetic defined medium, treated with either 10uM NaOH (Mock) or with the addition of indicated concentrations of CK (6-Benzylaminopurine). Cells were incubated at 30°C for 25h, with continuous shaking. Average growth per time point for 3 experiments is presented, N=9. Blue color represents statistical significance from Mock treatment in a two-tailed t-test with Holm-Sidak correction, p<0.05. **(b)** Average growth (OD) at mid log phase (15h) in three independent experiments. Letters indicate significance in a one-way ANOVA with a post hoc Tukey test; p<0.0001. All points displayed; red lines indicate mean ±SE.

(c-f) *S.cerevisiae* yeast cells were grown overnight at 30°C in YPD medium, diluted (OD$_{600}$ = 0.2) and incubated for 6 hours in YPD media (Mock) or media supplemented with 300 µM CK (6-Benzylaminopurine). Cells were incubated with 24 µM FM4-64 (Invitrogen) at 4°C for 30 min. Subsequently, the FM4-64 containing medium was replaced with fresh medium and cultures was incubated at 28°C for 15 minutes. Confocal microscopy images were acquired using a Zeiss LSM780 confocal microscope. **(c)** cell size; **(d)** total internalized FM4-64 per cell represented by pixel intensity; **(e)** endosome density. **(f)** Representative images, Bar, 10 µm. Box-plots with all values displayed; line indicates median. **c-e:** N>160. Image analysis was performed using Fiji-ImageJ with raw images collected from 3 independent biological experiments. Endosome count measurements were done with the 3D Object counter tool and pixel intensity was measured using the measurement analysis tool. Asterisks represent statistical significance in a two-tailed t-test with a Mann-Whitney post hoc test, *p<0.05, ****p<0.0001.

Fig. 10. Cytokinin mediated growth inhibition is partially rescued in budding yeast endocytic mutants.

S. cerevisiae Wild-type (WT, a-f), *ypt31Δ* (**a,e,f**)*, ssa1Δ* (**b,e,f**)*, vps1Δ* (**c,e,f**) and *spo14Δ* (**d,e,f**) were grown over night at 30°C for 25 h, in minimal synthetic defined medium, treated with either 10 µM NaOH (Mock) or with the addition of 300 µM (**a-e**) or 500 µM (**f**) CK (6-Benzylaminopurine).

924   **(a-d)** Average growth per time point for three experiments is presented, N=9. Asterisks indicate

925   statistical significance of each mutant with CK compared to WT with CK, in a two-tailed t-test with

926   Holm-Sidak correction, *$p < 0.05$, **$p < 0.01$, ***$p < 0.001$, ****$p < 0.0001$.

927   **(e-f)** Percentage of growth inhibition of each strain with 300µM CK (e) and 500 µM CK (f) as

928   compared to mock treatment, at 13 h, in three independent experiments, N=9. Boxplots are shown

929   with inter-quartile-ranges (box), medians (black line in box), and outer quartile whiskers, minimum

930   to maximum values. Asterisks indicate significance in a one-way ANOVA with a post hoc Tukey

931   test; *$p < 0.05$; **$p < 0.01$; ***$p < 0.001$; ns (non-significant).

932
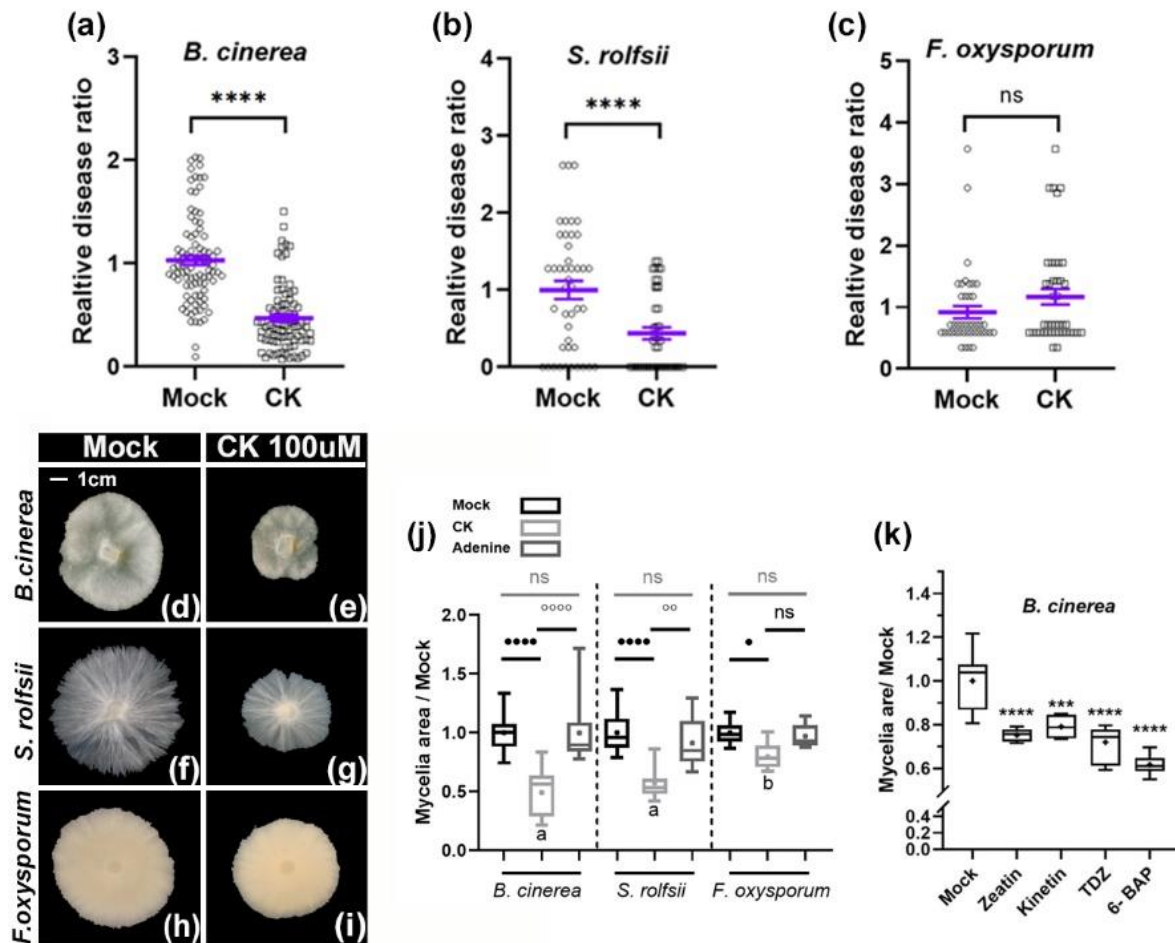
Fig. 1. Direct effect of cytokinin on fungal growth and disease.

(a)-(c) *S. lycopersicum* cv M82 leaves were treated with 100 µM CK (6-BAP; 6-Benzylaminopurine) and inoculated with indicated pathogens 24 hours later. Plant disease was quantified as indicated in the material and methods section, disease in the mock treatment was set to 1. Graphs represent results from 4-6 biological repeats ±SE, N>40. Asterisks represent significant difference among means in a two-tailed t-test, ****$p < 0.0001$, ns-non-significant. All individual values plotted, purple bar represents mean ±SE.

(d)-(i) *B. cinerea, S. rolfsii and F. oxysporum* were cultured on potato dextrose agar (PDA) plates in the presence of 100 µM 6-BAP. **(j)** Quantification of results from 4-6 biological repeats ±SE, including adenine (100 µM) as a control, N>20. Asterisks (differences between Mock and CK) and letters (differences between the level of CK growth inhibition in the different fungi) indicate significance in one-way ANOVA with a Bonferroni post hoc test, *$p < 0.05$, **$p < 0.01$, ****$p < 0.0001$, ns=non-significant. **(k)** *B. cinerea* was cultured on potato dextrose agar (PDA) plates in the presence of 100 µM of the indicated CK compound (TDZ=Thidiazuron). Quantification of results from 3 biological repeats ±SE, N=12. Asterisks indicate significance in one-way ANOVA with a Tukey post hoc test, ***$p < 0.001$, ****$p < 0.0001$. **(i-k)** Dose response of *B. cinerea, S. rolfsii and F. oxysporum* to CK-different concentrations of 6-BAP as indicated. Graphs represent 3 biological repeats ±SE, N>6. Letters

40

indicate significance in a one-way ANOVA, ****p<0.0001 in all cases, with a Tukey post-hoc test. **j-k**: Box-plot displays minimum to maximum values, with inner quartile ranges indicated by box and outer-quartile ranges by whiskers. Line indicates median, dot indicates mean.
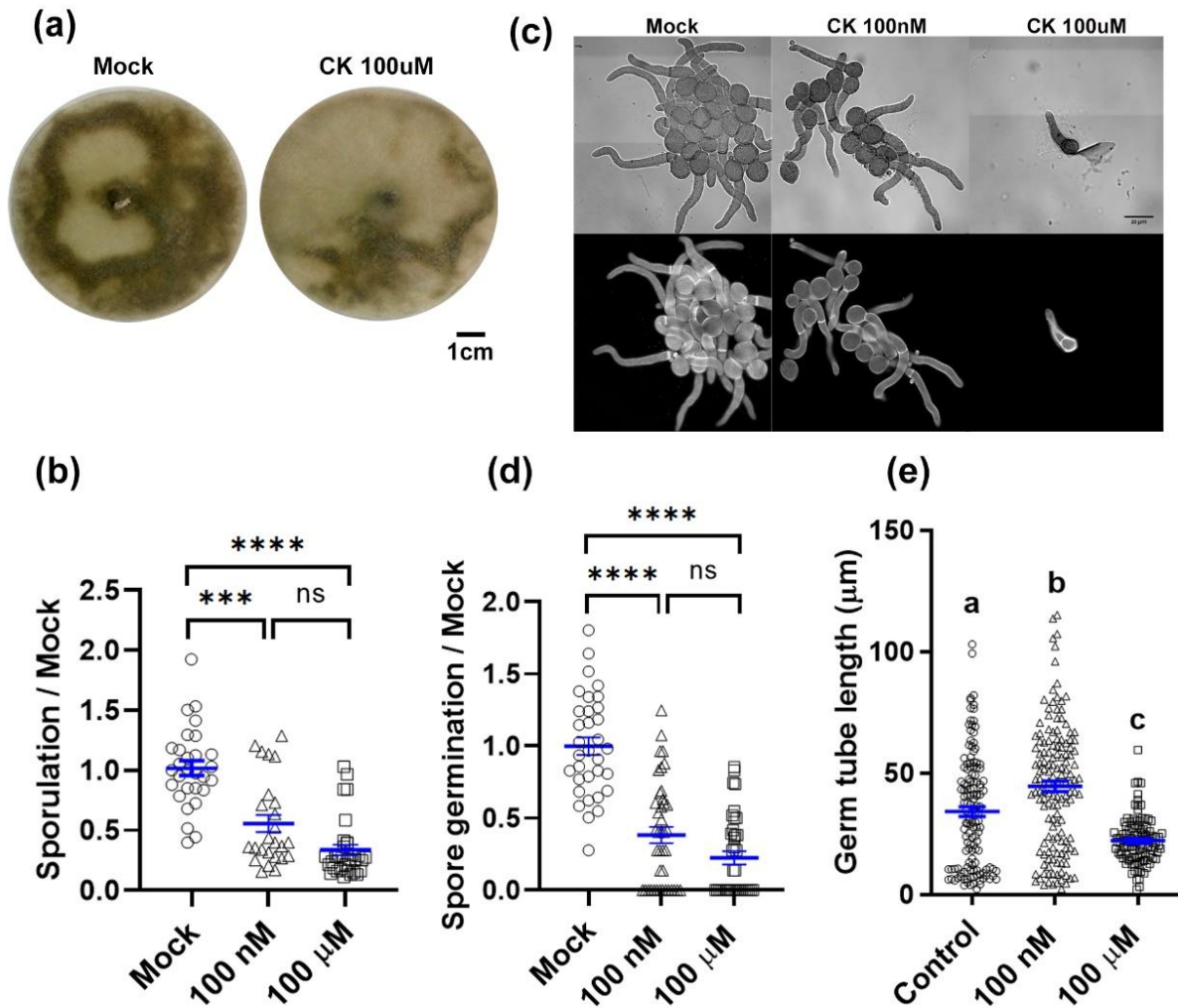
Fig. 2. Cytokinin inhibits *Bc* sporulation and spore germination.

(a)-(b) *B. cinerea* was cultured on PDA plates or PDB liquid broth in the presence of 100 nM or 100 µM 6-Benzylaminopurine (6-BAP). Spore formation is indicated by dark color **(a)** and quantified in **(b)**. Spore germination and germ tube elongation are demonstrated in **(c)** with calcofluor staining (scale bar = 20 µM), and quantified in **(d)-(e)**. **(b,d,e)** Quantification of results from 4 biological repeats ±SE, N>25. Asterisks or letters indicate significance in one-way ANOVA with a Tukey post hoc test, ***p<0.005, ****p<0.001. Individual values graphed, blue bar represents mean ±SE.
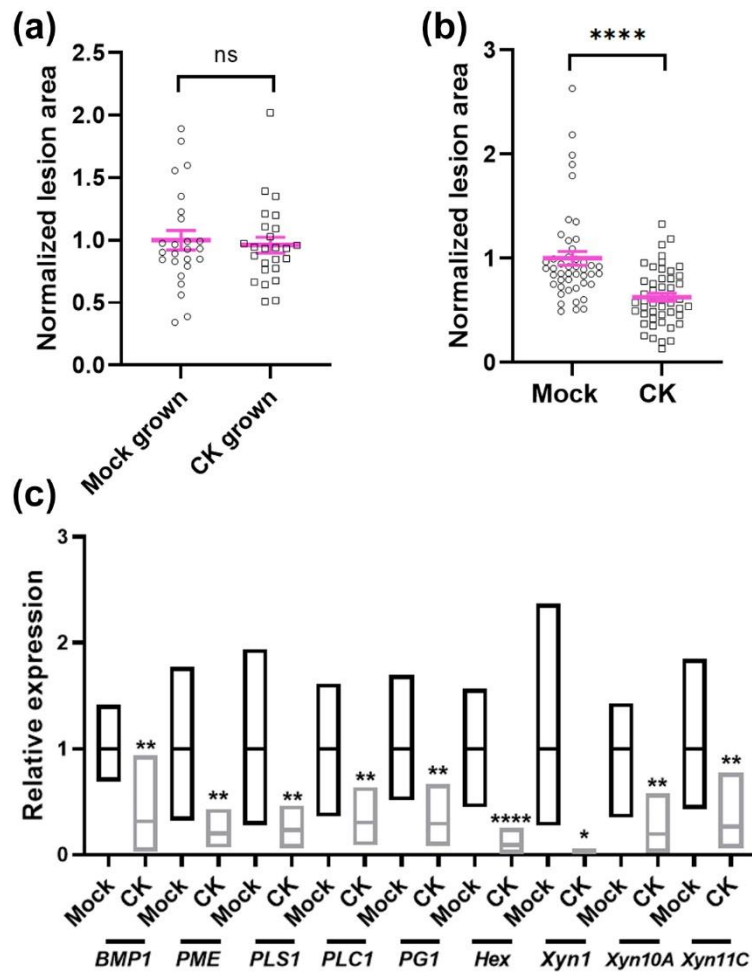
Fig. 3. Cytokinin inhibits *B. cinerea* virulence.

(a) Infectivity of spores sporulated from mycelia grown with or without cytokinin (CK; 6-Benzylaminopurine). Spores were harvested in a glucose/potassium media as described in the materials sections, and diluted to an equal concentration (the CK grown spores were concentrated as CK grown fungi produce reduced numbers). **(b)** Infectivity of spores grown in rich media and harvested from the same plate; half the spores were mixed with CK prior to infection. **(c)** *B. cinerea* was grown in PDB with the addition of 100 µM CK (6-BAP) or without (Mock). qRT-PCR was carried out on the virulence genes *BMP1, PME, PLS1, PLC1, PG1, hex, XynI, Xyn10A* and *Xyn11C*. Mock was set to 1. Gene expression values were normalized to a geometric mean of the expression of 3 housekeeping genes: Ubiquitin-conjugating enzyme E2, Iron-transport multicopper oxidase, and Adenosine deaminase. Graph represents 3 biological repeats, N=9. **a-b:** individual values graphed, pink bar represents mean ±SE. Results were analyzed for statistical significance using a two-tailed t-test, ****$p<0.0001$; ns-non-significant. **c:** floating bars, line indicates mean. Results were analyzed for statistical significance using Welch's Anova with a Dunnett post hoc test, *$p<0.05$, **$p<0.01$, ****$p<0.0001$.
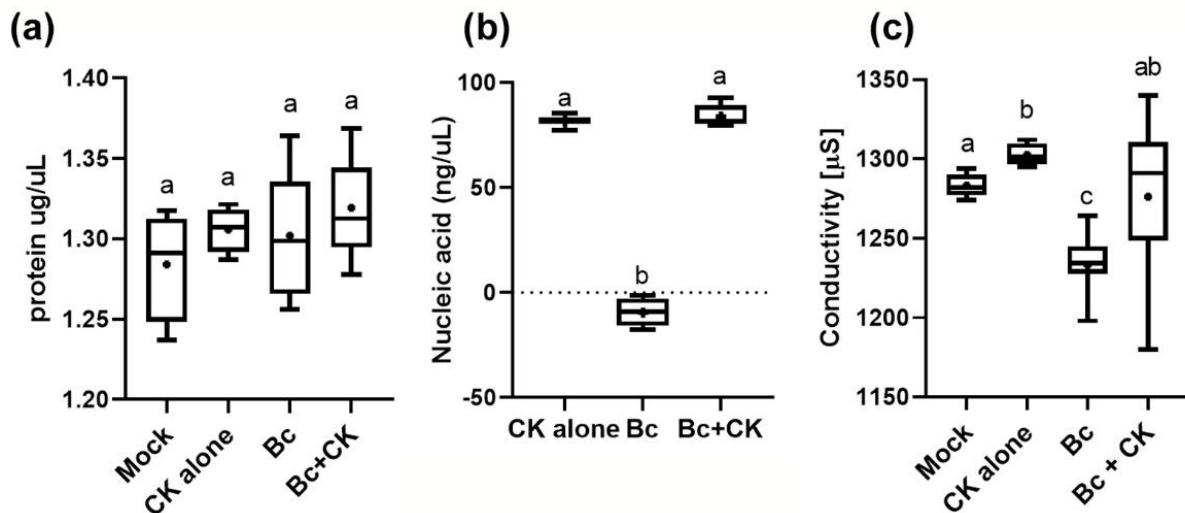
Fig. 4. Cytokinin is not toxic to *B. cinerea*.

B. cinerea (*Bc*) was cultured in PDB liquid broth, with or without 100 µM CK (6-Benzylaminopurine). After 24 hours, protein leakage **(a)**, nucleic acid leakage **(b)**, and media conductivity **(c)** were measured. Graphs represent 3 biological repeats ±SE, N>6. Letters indicate significance in one-way ANOVA with a Tukey (a) or Bonferroni (b,c) post hoc test; a p=ns; b,c p<0.0001. Box-plot with 2.5% whiskers; line indicates median, dot indicates mean. No significant difference between control media containing CK (without *Bc*) or *Bc* with CK was observed in any of the parameters.
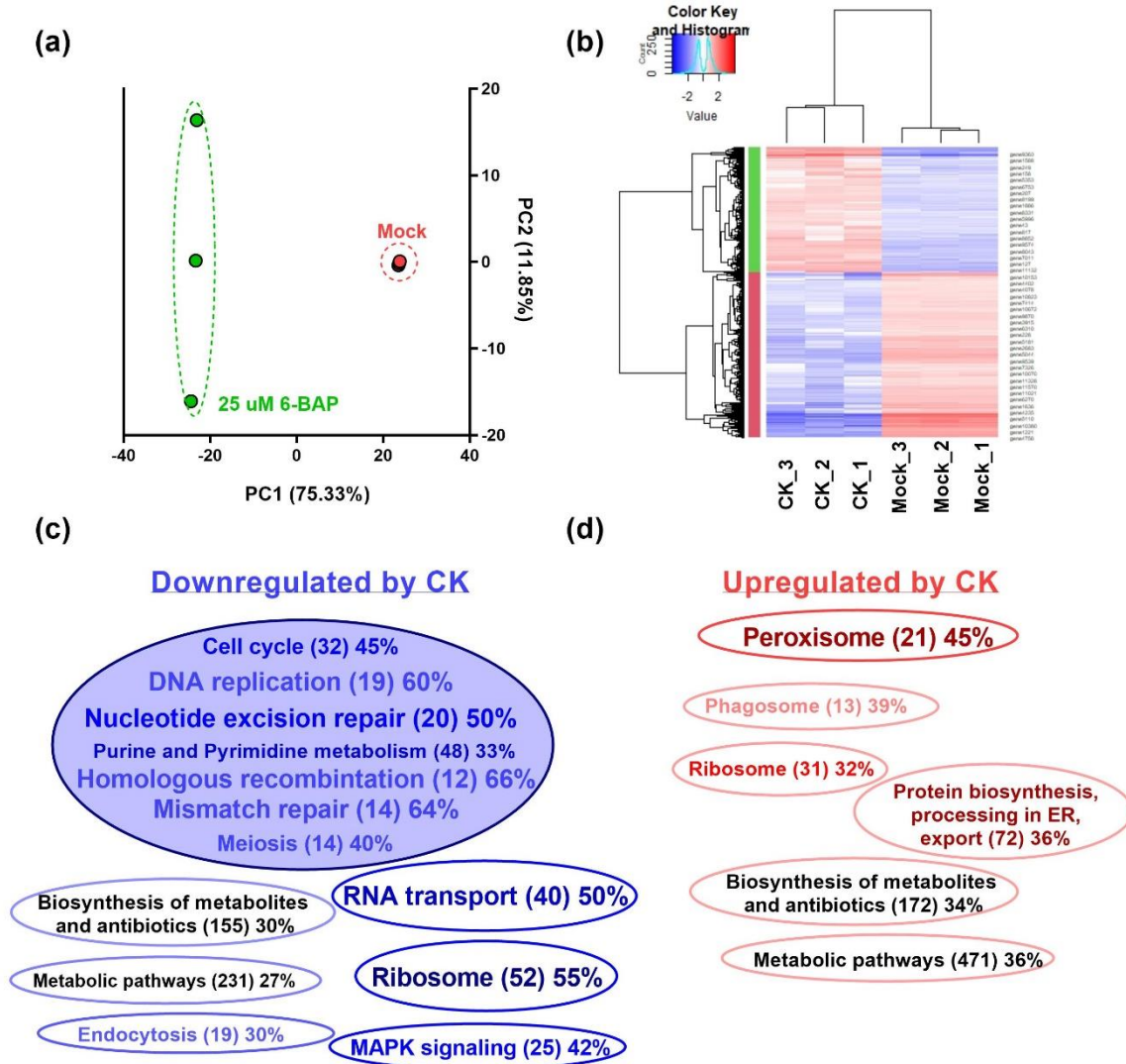
44

Fig. 5. Transcriptomics reveal fungal pathways affected by CK

Analysis of Illumina Hiseq NGS of *Bc* samples Mock treated or CK treated (25 uM), 3 biological repeats each. Gene expression values were computed as FPKM. Differential expression analysis was completed using the DESeq2 R package. Genes with an adjusted p-value of no more than 0.05 and log2FC greater than 1 or lesser than -1 were considered differentially expressed. **(a)** Principle component analysis (PCA) of 3 biological repeats from each treatment. PCA was calculated using the R function prcomp. **(b)** Heatmap depicting the clustering of the different samples in terms of differentially expressed genes. Blue= negatively regulated by CK, red= positively regulated by CK. Color saturation indicates strength of differential expression. Heatmap visualization was performed using R Bioconductor. See also Supplemental data 1. **(c-d)** Analysis of statistically enriched pathways downregulated (c, blue) and upregulated (d, red) by CK. KOBAS 3.0 tool was used to detect the statistical enrichment of differential expression genes in Kyoto Encyclopedia of Genes and Genomes (KEGG) pathways and Gene Ontology (GO). Pathways were tested for significant enrichment using Fisher's exact test, with Benjamini and Hochberg FDR correction. Corrected p-value was deemed

45

significant at p<0.05. See also Supplemental data 2 and 3. In (c-d), the darker the color the higher the number of DEGs in a pathway, and the bigger the letters, the higher percentage of the pathway that is differential.
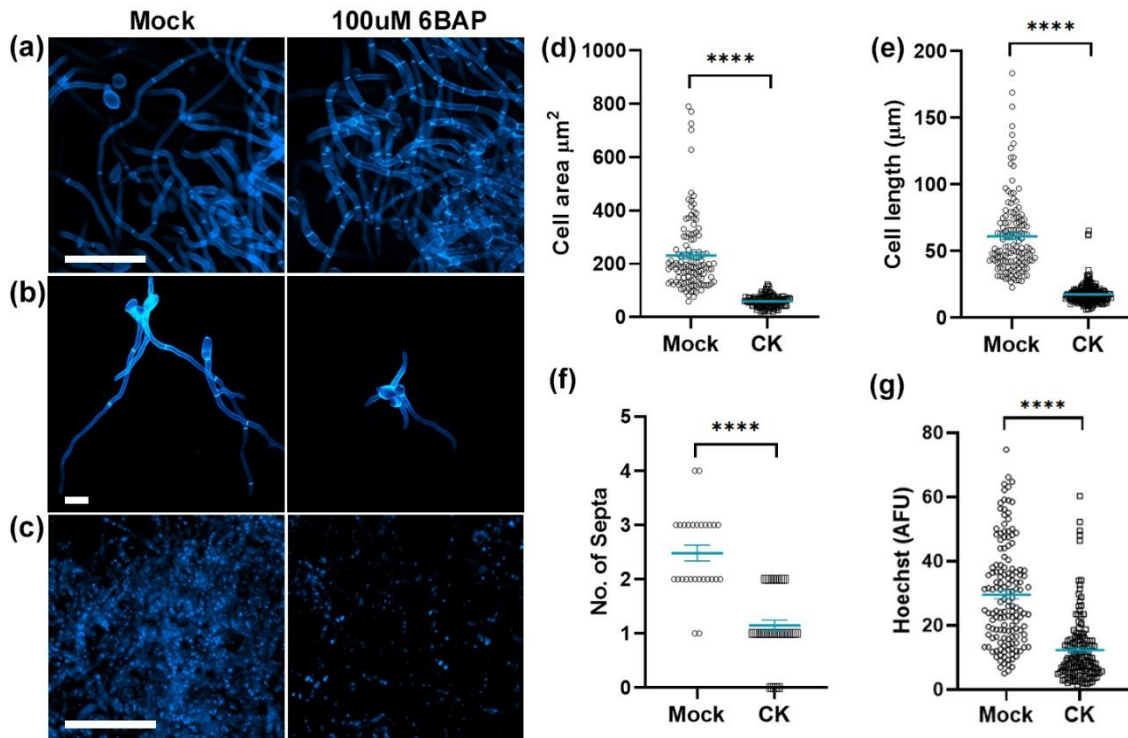
Fig. 6. Cytokinin reduces *B. cinerea* cell elongation and DNA replication

B. cinerea was cultured in PDB liquid broth, with or without 100 µM CK (6-Benzylaminopurine). After 8 **(f)** or 16 hours **(a-e,g)**, growing hyphae were stained with calcofluor **(a,b,d,e,f)** or hoechst **(c,g)**, and imaged on an Olympus IX 81 confocal laser scanning microscope using a 405nm diode laser (1% power), under identical imaging conditions. **a-c:** bar=50 µM; **b:** bar=20 µM. Cell area **(d)**, distance between septa **(e)**, No. of septa in individual germinated hyphae **(f)** and DNA staining **(g)** were measured using Fiji-ImageJ. Graphs represent 3-6 biological repeats, N>120 (d,e), N>30 (f), N=170 (g). Statistically significant differences between Mock and CK samples were assessed using a two-tailed t-test, ****p<0.0001. Individual values graphed, blue bar represents mean ±SE.
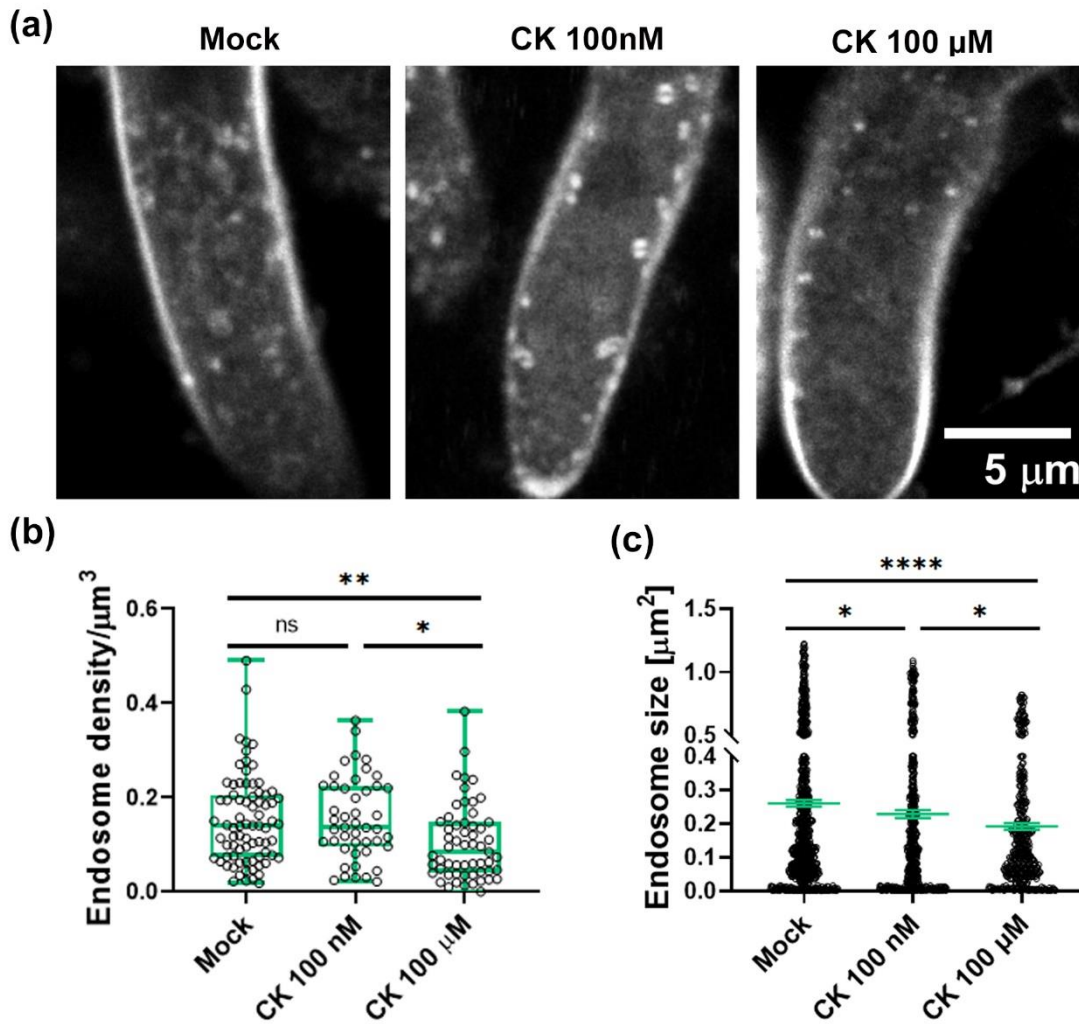
47

Fig. 7. Cytokinin inhibits the fungal cytoskeleton

(a) Cytoskeleton related *B. cinerea* genes found to be differentially regulated in the RNAseq. See Supplemental data 4 for full list. (b) qRT-PCR validation of expression levels of 5 cytoskeleton related genes upon CK treatment. *B. cinerea* was grown in PDB with the addition of 100 µM CK (6-BAP) or without (Mock). Mock was set to 1. Gene expression values were normalized to a geometric mean of the expression of 3 housekeeping genes: Ubiquitin-conjugating enzyme E2, Iron-transport multicopper oxidase, and Adenosine deaminase. Floating bars represent minimum to maximum values of 3 biological repeats, line represents mean. Asterisks indicate significance in a two-tailed t-test with Welch's correction, *p<0.05; ***p<0.001. (c-d) *B. cinerea* was transformed with lifeactin-GFP. Germinated spores were treated with Mock or CK and grown for 6 h prior to confocal visualization. (c) Representative images, bar=10 uM. (d) Analysis of corrected total fluorescence (CTF) of the ratio between life-actin at the tip of the cell and the total cell in Mock and CK treated cells. Three independent experiments were conducted with a total of 30 images analyzed, N>80 growing hyphae tips. Asterisks indicate significance in a two-tailed t-test with Welch's correction, ****p<0.0001.

Fig. 8. Cytokinin inhibits FM-4-64 endocytosis in growing *B. cinerea* hyphae.

B. cinerea (*Bc*) was cultured in PDB liquid broth in the presence of 100 nM or 100 µM CK (6-Benzylaminiopurine) for 16 hours. **(a)** FM-4-64 endocytic vesicles in *Bc* hyphae. **(b)** quantification of the amount of endocytic vesicles; **(c)** quantification of the average size of vesicles. Measurements were done using the counting tool of Fiji. Quantification of results from 7 biological repeats. **b:** N>45, box-plot with all values displayed, box indicates inner-quartile ranges with line indicating median, whiskers indicate outer-quartile ranges. **c:** N>450, all values displayed, line indicates median ±SE. Asterisks indicate significance in one-way ANOVA with a Tukey post hoc test, *$p < 0.05$; **$p < 0.01$; ****$p < 0.0001$; ns- non-significant.

Fig. 9. Cytokinin inhibits growth and endocytosis in budding yeast.

(a) Wild-type *Saccharomyces cerevisiae* were grown over night at 30°C in minimal synthetic defined medium, treated with either 10uM NaOH (Mock) or with the addition of indicated concentrations of CK (6-Benzylaminopurine). Cells were incubated at 30°C for 25h, with continuous shaking. Average growth per time point for 3 experiments is presented, N=9. Blue color represents statistical significance from Mock treatment in a two-tailed t-test with Holm-Sidak correction, p<0.05. **(b)** Average growth (OD) at mid log phase (15h) in three independent experiments. Letters indicate significance in a one-way ANOVA with a post hoc Tukey test; p<0.0001. All points displayed; red lines indicate mean ±SE. **(c-f)** *S.cerevisiae* yeast cells were grown overnight at 30°C in YPD medium, diluted (OD$_{600}$ = 0.2) and incubated for 6 hours in YPD media (Mock) or media supplemented with 300 µM CK (6-Benzylaminopurine). Cells were incubated with 24 µM FM4-64 (Invitrogen) at 4°C for 30 min. Subsequently, the FM4-64 containing medium was replaced with fresh medium and cultures was incubated at 28°C for 15 minutes. Confocal microscopy images were acquired using a Zeiss LSM780 confocal microscope. **(c)** cell size; **(d)** total internalized FM4-64 per cell represented by pixel intensity; **(e)** endosome density. **(f)** Representative images, Bar, 10 µm. Box-plots with all values displayed; line indicates median. **c-e:** N>160. Image analysis was performed using Fiji-ImageJ with raw images collected from 3 independent biological experiments. Endosome count measurements were done with the 3D Object counter tool and pixel intensity was measured using the measurement analysis tool. Asterisks represent statistical significance in a two-tailed t-test with a Mann-Whitney post hoc test, *p<0.05, ****p<0.0001.
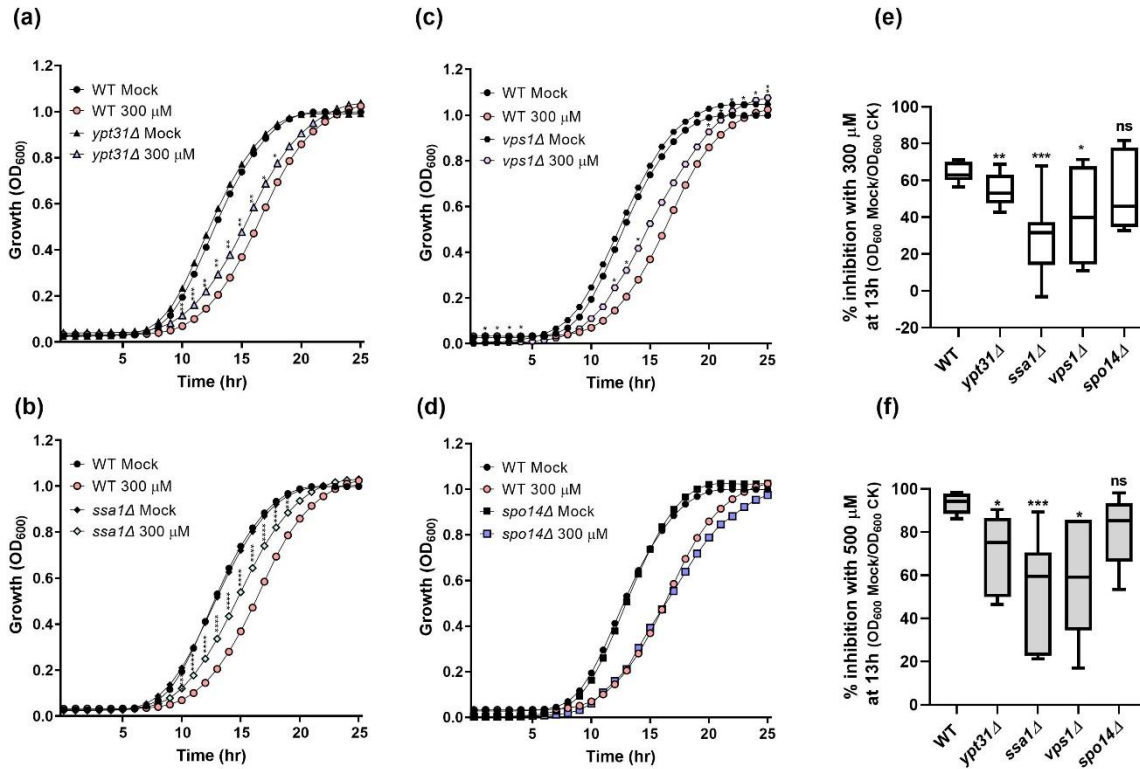
Fig. 10. Cytokinin mediated growth inhibition is partially rescued in budding yeast endocytic mutants.

S. cerevisiae Wild-type (WT, a-f), *ypt31Δ* (**a,e,f**)*, ssa1Δ* (**b,e,f**)*, vps1Δ* (**c,e,f**) and *spo14Δ* (**d,e,f**) were grown over night at 30°C for 25 h, in minimal synthetic defined medium, treated with either 10 µM NaOH (Mock) or with the addition of 300 µM (**a-e**) or 500 µM (**f**) CK (6-Benzylaminopurine).

(a-d) Average growth per time point for three experiments is presented, N=9. Asterisks indicate statistical significance of each mutant with CK compared to WT with CK, in a two-tailed t-test with Holm-Sidak correction, $*p<0.05$, $**p<0.01$, $***p<0.001$, $****p<0.0001$.

(e-f) Percentage of growth inhibition of each strain with 300µM CK (e) and 500 µM CK (f) as compared to mock treatment, at 13 h, in three independent experiments, N=9. Boxplots are shown with inter-quartile-ranges (box), medians (black line in box), and outer quartile whiskers, minimum to maximum values. Asterisks indicate significance in a one-way ANOVA with a post hoc Tukey test; $*p<0.05$; $**p<0.01$; $***p<0.001$; ns (non-significant).

Cytokinin inhibits fungal development and virulence by targeting the cellular cytoskeleton and trafficking
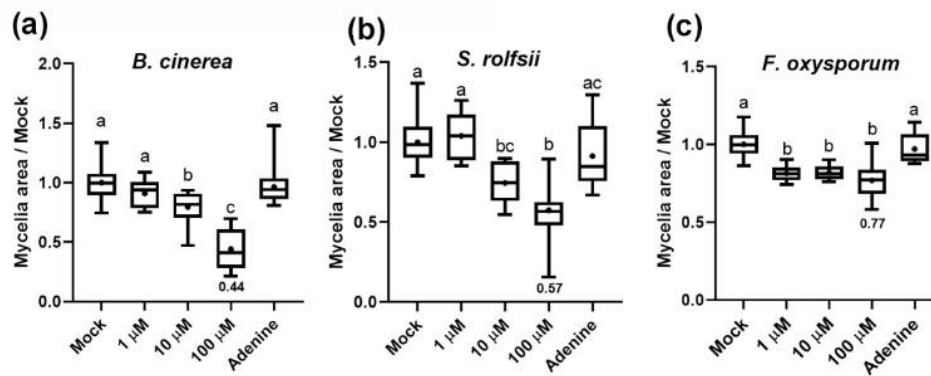
Supplemental Information

Fig. S1. Direct effect of cytokinin on mycelial growth of phytopathogenic fungi: 6-BAP dose response

Dose response of *B. cinerea* (**a**), *S. rolfsii* (**b**) and *F. oxysporum* (**c**) to CK- different concentrations of 6-Benzylaminopurine as indicated. Graphs represent 3 biological repeats ±SE, N>6. Letters indicate significance in a one-way ANOVA, ****$p<0.0001$ in all cases, with a Tukey post-hoc test. Box-plot displays minimum to maximum values, with inner quartile ranges indicated by box and outer-quartile ranges by whiskers. Line indicates median, dot indicates mean.
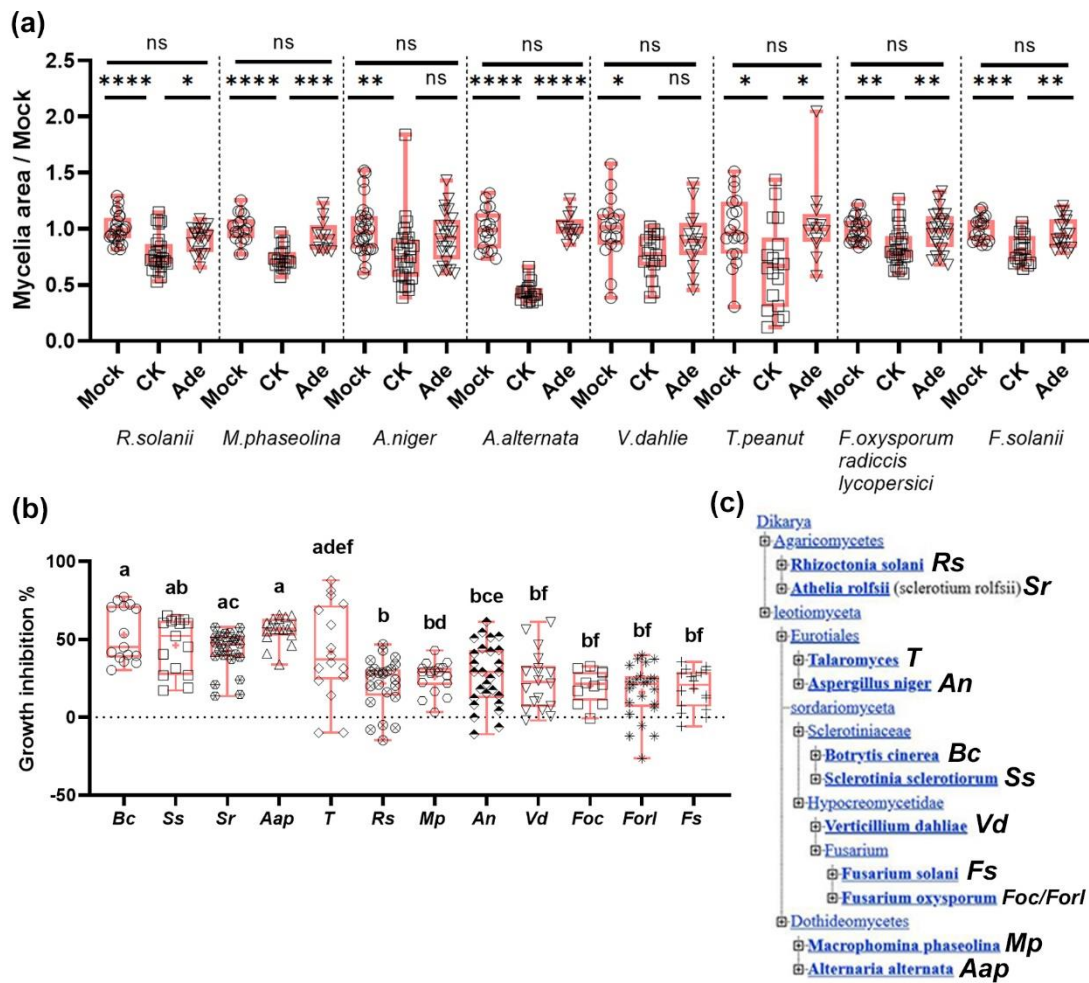
Fig. S2. Cytokinin inhibits fungal growth.

(a) Growth of different fungi cultured on potato dextrose agar (PDA) plates in the presence of 100 µM CK (6-Benzylaminopurine), or the control Adenine (Ade). Quantification of results from 4-6 biological repeats ±SE, N>12. Asterisks indicate significance in one-way ANOVA with a Tukey post hoc test, *p<0.05, **p<0.01, ***p<0.001; ****p<0.0001; ns (non-significant). **(b)** Comparison of the inhibition level of CK for different fungi. Letters indicate significance in a two-tailed t-test, p<0.004. The phylogeny is detailed in **(c)**. **a-b:** Box plots with all individual values shown, line indicates median.
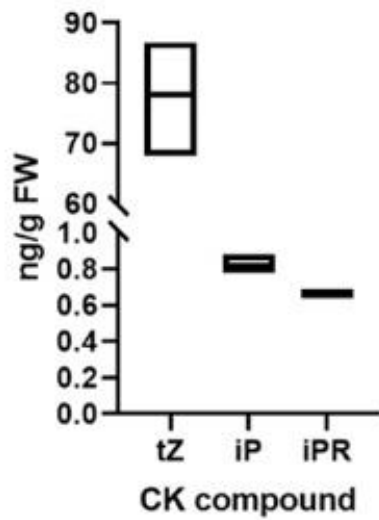
53

Fig. S3. Quantification of active CKs in tomato leaves using LC–MS-MS.

Fresh ground tissue powder was iso-propanol/methanol extracted in the presence of deuterium-labelled internal standards. LC–MS-MS analyses were conducted using a UPLC-Triple Quadrupole MS (WatersXevo TQMS). Acquisition of LC–MS data was performed using Mass Lynx V4.1 software (Waters). Quantification of CKs (tZ, trans zeatin, iP, isopentenyladenine and iPR, iP riboside) was done using isotope-labeled internal standards (IS), as described in the methods section. Quantification of results from 3 biological replicas ±SE. Bars represent minimum-maximum values range, with line indicating mean.
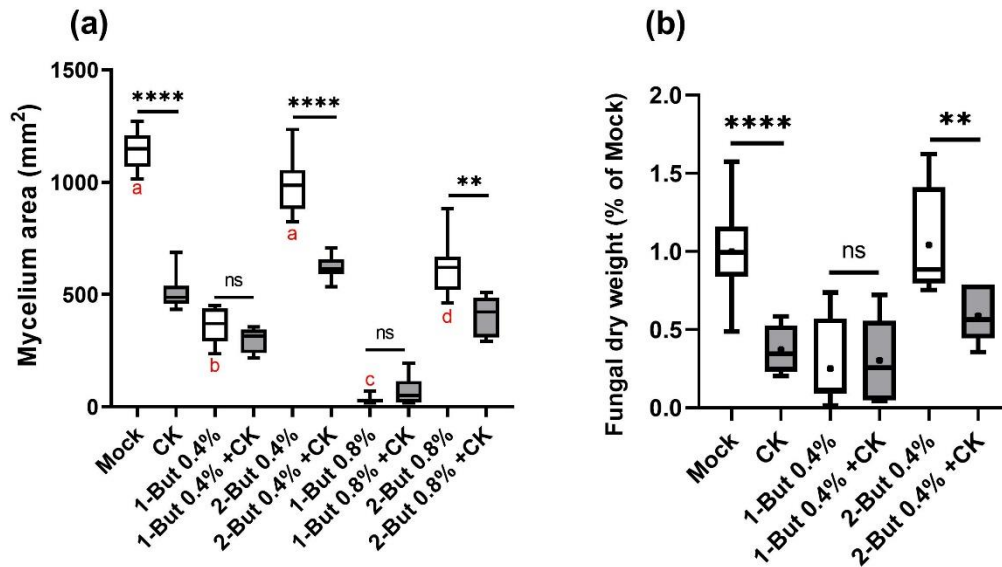
Fig. S4. Inhibition of endocytosis abolishes *B. cinerea* cytokinin sensitivity

B. cinerea was cultured on 1/2 PDA plates (a) or in PDB liquid broth (b) in the presence or absence of 100 µM CK (6-Benzylaminopurine), the endocytosis inhibitor 1-butanol (v/v%), or control compound 2-butanol (v/v%) for 48 (a) or 96 (b) hours. **(a)** Mycelium area; measurements were done using Fiji. **(b)** Dry weight %. Quantification of results from 4 biological repeats ±SE, a: N>6, b: N>9. Boxplots are shown with inter-quartile-ranges (box), medians (black line in box), means (dot) and outer quartile whiskers, minimum to maximum values. Asterisks indicate significance in one-way ANOVA with a Dunnett post hoc test, **p<0.01; ****p<0.0001; ns (non-significant). Red letters in (a) indicate significance between the different treatments without CK in a one-way ANOVA with a Dunnett post hoc test, p<0.01.
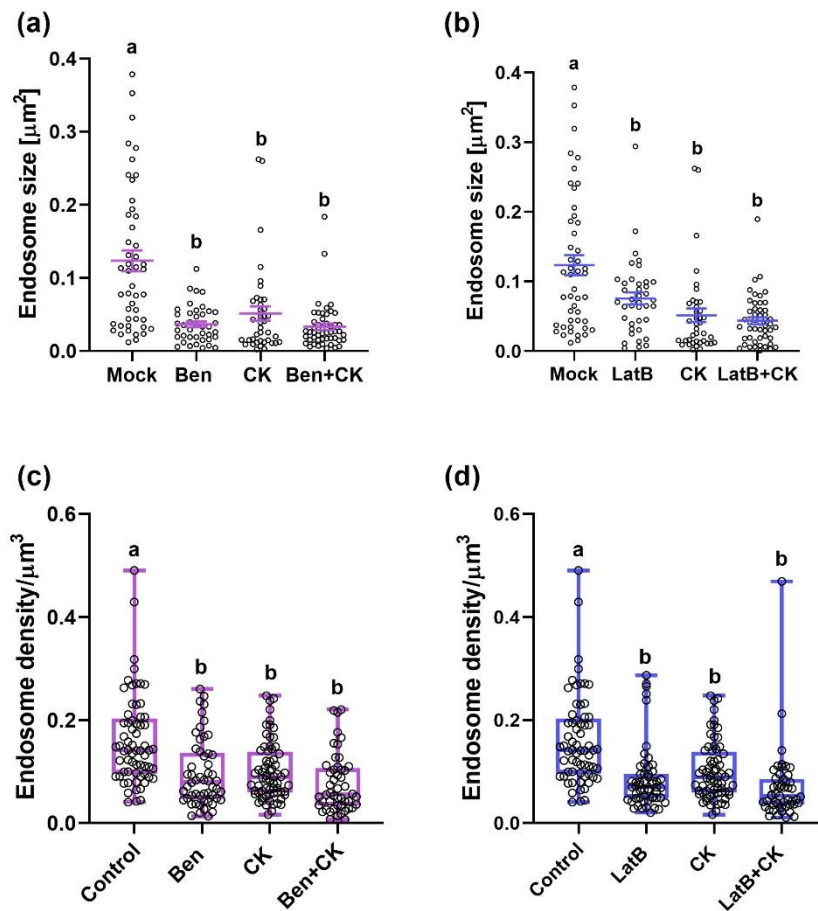
Fig. S5. Inhibition of the cellular cytoskeleton abolishes *B. cinerea* cytokinin sensitivity-cellular trafficking

B. cinerea (*Bc*) was cultured in PDB liquid broth in the presence of 100 µM CK (6-Benzylaminiopurine) and/ or 1 uM Benomyl (Ben; **a,c**) or Latrunculin B (LatB; **b,d**) for 8 hours. FM-4-64 endocytic vesicles were analyzed in growing hyphae. Measurements were done using the counting tool of Fiji. **(a,b)** Quantification of the average size of vesicles from 3 biological repeats, N>40 images, the average endosome size per image was used for the analysis. All points displayed, mean ±SE is indicated. **(c,d)** Quantification of the amount of endocytic vesicles from 5 biological repeats, N>50 images. Box-plots with all values displayed, box indicates inner-quartile ranges with line indicating median, whiskers indicate outer-quartile ranges. Different letters indicate significance between samples in a one-way ANOVA with a Dunnett post hoc test, a,b: p<0.0059; c,d: p<0.0001.
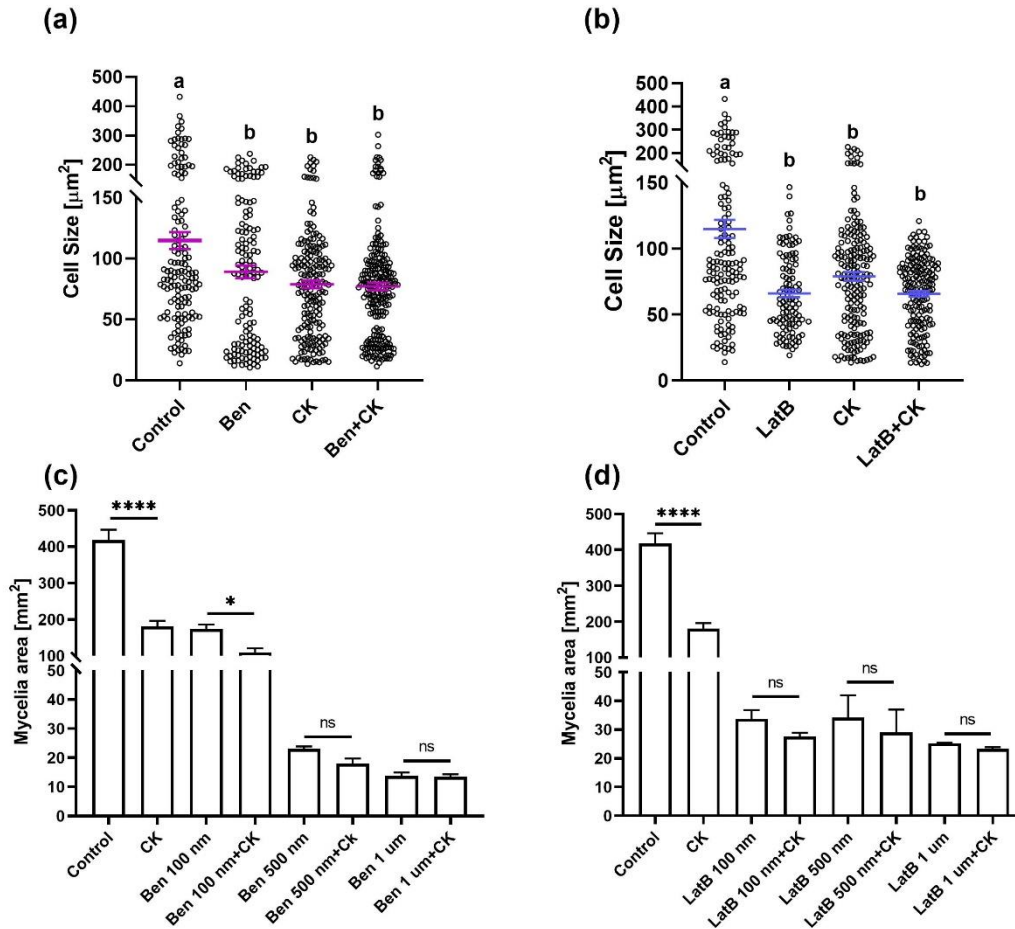
Fig. S6. Inhibition of the cellular cytoskeleton abolishes *B. cinerea* cytokinin sensitivity-cell cycle and growth

(a-b) *B. cinerea* (*Bc*) was cultured in PDB liquid broth in the presence of 100 µM CK (6-Benzylaminiopurine) and/ or 1 uM Benomyl (Ben; **a**) or Latrunculin B (LatB; **b**) for 8 hours. Cell size was quantified in 3 experiments, N>100. All points displayed, mean ±SE is indicated. Different letters indicate significance between samples in a one-way ANOVA with a Dunnett post hoc test, p<0.021.

(c-d) *B. cinerea* (*Bc*) was cultured on PDA plates in the presence of 100 µM CK (6-Benzylaminiopurine) and/ or indicated concentrations of Benomyl (Ben; **c**) or Latrunculin B (LatB; **d**) for 48 hours. Graph represents mean ±SE, N=3. Asterisks indicate significance between samples in a one-way ANOVA with a Bonferroni post hoc test, *p<0.05; ****p<0.0001; ns=not significant.
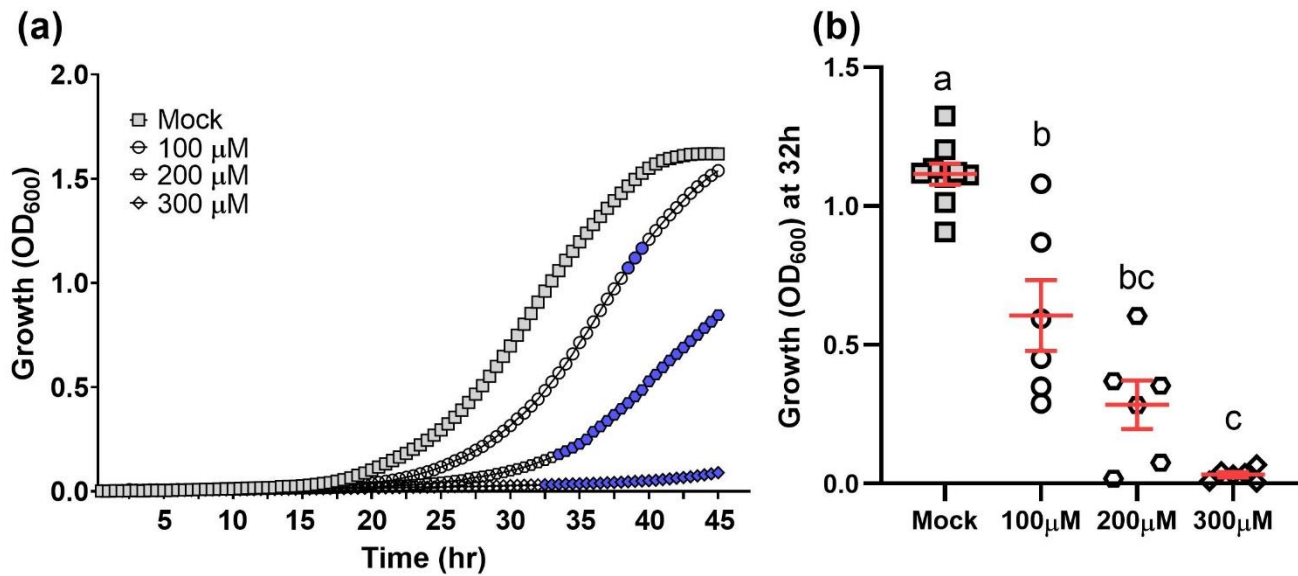
.

Fig. S7. Cytokinin inhibits the growth of fission yeast.

(a) Wild-type *Schizosaccharomyces pombe* cells were grown over night at 30°C in minimal EMM medium, treated with either 10uM NaOH (Mock) or with the addition of indicated concentrations of CK (6-Benzylaminopurine). Cells were incubated at 30°C for 45h, with continuous shaking. Average growth per time point for three independent experiments is presented, N=6. Blue color represents statistical significance in a two-tailed t-test with Holm-Sidak correction, $p < 0.05$. (b) Average growth (OD) at mid log phase (32h) in three independent experiments. Letters indicate significance in a one-way ANOVA with a post hoc Tukey test; $p < 0.0001$. All points displayed; red lines indicate mean ±SE.
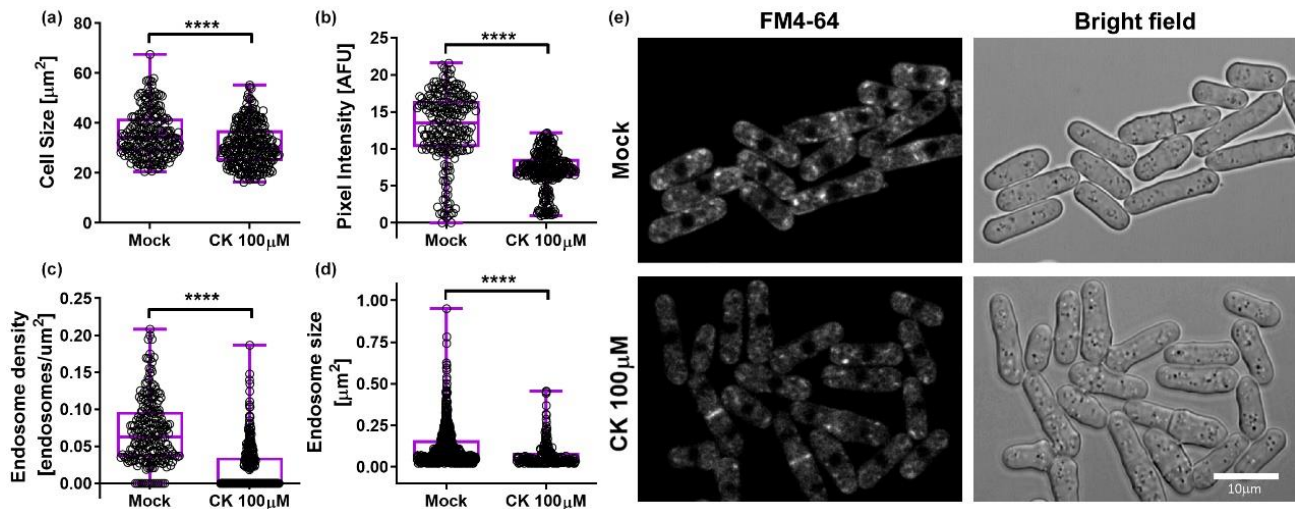
Fig. S8. Cytokinin inhibits FM-4-64 endocytosis in fission yeast.

S. pombe were grown overnight at 30°C in YE medium, diluted (OD_{600} = 0.2) and incubated for 6 hours in YE medium (Mock) or medium supplemented with 100 µM CK (6-Benzylaminopurine). Cells were incubated with 24 µM FM4-64 (Invitrogen) at 4°C for 30 min. Subsequently, the FM4-64 containing medium was replaced with fresh medium and cultures was incubated at 28°C for 15 minutes. Confocal microscopy images were acquired using a Zeiss LSM780 confocal microscope system with Objective LD C-Apochromat 63×/1.15 Corr. Acquisition settings were designed using an excitation laser wavelength of 514 nm (4% power). The emission was then collected in the range of 592–768 nm. Bright field was acquired using the T-PMT (transmitted light detector). **(a)** cell size; **(b)** total internalized FM4-64 per cell represented by pixel intensity; **(c)** endosome density; **(d)** endosome size. **(e)** Representative images, Bar, 10 µm. Box-plots with all values displayed; line indicates median. **a-c:** N>220; **d:** N>180. Image analysis was performed using Fiji-ImageJ with raw images collected from 3 independent biological experiments. Endosome count and size measurements were done with the 3D Object counter tool and pixel intensity was measured using the measurement analysis tool. Asterisks represent statistical significance in a two-tailed t-test with a Mann-Whitney post hoc test, ****$p<0.0001$.

59

Supplementary Table 1

Solvent gradients and MS-MS parameters for CK quantification.

Solvent gradient program for cytokinins:

Time (min)	Phase A %	Phase B %
Initial	95	5
0.5	95	5
14	50	50
15	5	95
18	5	95
19	95	5
22	95	5

LC-MS-MS parameters for quantifications:

Analite and IS	Retention time (min)	Ionization Mode	MRM transition (m/z)	Dwell time (msec)	Cone (V)	Collision (V)
t-Z	2.34	positive	220>202 220>136	78	26	14 18
^{2}H5-t-Z	2.35	positive	225>137 225>207	78	22	18 12
iP	4.86	positive	204>136 204>69	30	20	14 16
^{2}H6-iP	4.82	positive	210>137 210>75	30	24	16 18

60

Supplementary Table 2

Primers used in RT-qPCR.

Gene	Sequence (5'-3')	Primer Efficiency
PG1	F-GATGTTGGTTCCTCCAGCGATA R-CCGGAGTTGATAGCGAGACAGT	1.03
BMP1	F-TCTTTCAATGTCAGCGAGCAA R-TGCAAAGCTGAGCAGACAACA	1.03
PLC1	F-TCCCGCAGGACTCGATAACT R-TATGGCTTCCACTCGGGTTT	0.98
PLS1	F-CGCCTTCCTCATCTCCATTC R-CAACGACGAAGAAGCCATGAA	1.03
PME1	F-GCCACCCAGTTCATCGGATA R-CCGACGACGAGACATTTAGCA	0.99
PutXyn11A	F-CTCATCGAATACTACATCGT R-GTATTGCTTGAAGGTAGCA	1.01
Xyn10A	F-GGAAAGATCTATGCATGGGATG R-AGGTTGCTGAATCCAGGTTG	1.03
Xyn11C	F-GAATCCTGGAAGTGCTAAGGC R-TGCTCCGTCACTAACCACG	1.01
hex	F-TCTACTTCAACGAGGCTTC R-CACCAGATTGACCGAAAAC	0.98
Tubulin alpha	F- TCTTGCTTCGAGCCCAAC R- ACAGCAGCGTGGACATCA	0.96
pfy1	F- ACCGCCGAGACTGTTCAA R- CCCACCACACATCATCCA	0.96
aft1	F- ATCTGGCTGGTGGCACAT R- CCCACCACACATCATCCA	1.00
sac6	F-CCTCAACCTGCCTCCTGA R-TCGCTCCCTTGTGTAGCC	1.02
smt	F-AGCACCAAACTCCGTTCG R-TAACTGCCAACGCAACGA	1.02
Ub (Ubiquitin)	F-CATCAACTCCAACGGAAGCA R-TCGGTCGGTCTTGTAAACGT	1.00
Iron transport multicopper oxidase	F-GTTTTTGGGACCGGCTTT R-GCCGCTTTTGAGGGAAAT	0.99
Adenosine deaminase	F-TGAGTGCCACGACGAAAA R-ACTCCACCATTGCCTCCA	1.02

Supplementary Table 3

Oligonucleotides used for generating and validating *Saccharomyces cerevisiae* mutant strains.

Primer	Sequence (5'-3')
YPT31_Disruption_Fw	GAATAACAATTTGACCTTTATTACAAGGCACTTTGTTTAGGCCAGCAAAGGGATTCTGACGGCGTCTGGGGATTTCAACAcggatccccgggttaattaa
YPT31_Disruption_Rev	AAAATTGTAAAAATATAGCACAGAATTAAAGGGGAGAAGAGTCATTCACATGCAAGTGCGCAACTGCTGCAAAATATCTCgaattcgagctcgtttaaac
YPT31_val_Fw	GTGCGGGTGCTAAATTAGAGA
YPT31_val_Rev	GATGAAGACGAAGAAGACGATG
SSA1_Disruption_Fw	TCTATTTGTAAGATAAGCACATCAAAAGAAAAGTAATCAAGTATTACAAGAAACAAAAATTCAAGTAAATAACAGATAATcggatccccgggttaattaa
SSA1_Disruption_Rev	AAAAACGTTCGGAAAATTCCTCATTATACCCAGATCATTAAAAGACATTTTCGTTATTATCAATTGCCGCACCAATTGGCgaattcgagctcgtttaaac
SSA1 _val_Fw	CTTCGAGAAGGGATTGAGTTG
SSA1 _val_Rev	GTAGCAGTACTTCAACCATTAG
VPS1_Disruption_Fw	TAAAAAAGAATTAGAGAGGCCTTTTATAGCACCAAAATAAGGACCGTACGAAAACTGCACATTTTATATT ATCAGATATCcggatccccgggttaattaa
VPS1_Disruption_Rev	CAATATATAAGATTTGCAGTAAATATTAGGGAGAAATACTCAAAACCAAGCTTGAGTCGACCGGTATAGATGAGGAAAACgaattcgagctcgtttaaac
VPS1_val_Fw	CGTCGCTTTGCCATCAAGAGA
VPS1_val_Rev	AGACTAGCTTCCACGTATAC

SPO14_Disruption_Fw	CGACCGGTCACTGATAATTCACACGACGCATTGAGAGGCACGTACGCAAGAAGAAAAGGTAGGATAGATAAACAAGGGTGcggatccccgggttaattaa
SPO14_Disruption_Rev	TATGTATCAGCGTCGAATGCTTATAACAGATAAAAGGAAAATACAGGTAATGGTGTGTTCCTGGTCGTTTTTATATTCCCgaattcgagctcgtttaaac
SPO14_val_Fw	GCAGGAC ATTATAGGCA CGA
SPO14_val_Rev	GCAATAATGACACTATGGACC

Supplementary Table 4

Oligonucleotides used for generating and validating *Botrytis cinerea* mutant strains.

Primer	Sequence (5'-3')
GA 34F	CGGGTGAATGGGATTCATTG
GA 34R	GCCCGCATTGGATTAATAATTG
GA 44F	GCCACAGACTCCGCCAGATTCTAATG
GA 44R	CAACCATTTCACGCTGCGACCACC
GA 31F	GCAACTAGTGATATTGAAGG
GA 31R	CATCTACTCTATTCCTTTGC